Evolution and transformation of the North Icelandic Irminger Current along the north Iceland shelf

Stefanie Semper[1], Kjetil Våge[1], Robert S. Pickart[2], Steingrímur Jónsson[3,4], and Héðinn Valdimarsson[4]

[1]Geophysical Institute, University of Bergen and Bjerknes Centre for Climate Research, Bergen, Norway
[2]Woods Hole Oceanographic Institution, Woods Hole, Massachusetts, USA
[3]University of Akureyri, Akureyri, Iceland
[4]Marine and Freshwater Research Institute, Hafnarfjörður, Iceland

Key Points:

- While propagating clockwise around north Iceland, the North Icelandic Irminger Current cools and freshens mainly because of lateral mixing.
- Baroclinic instabilities result in locally enhanced eddy kinetic energy over the slope northeast of Iceland.
- Dense water forms only sporadically on the north Iceland shelf; a significant contribution to the Denmark Strait overflow is questionable.

Corresponding author: Stefanie Semper, `stefanie.semper@uib.no`

Abstract

The North Icelandic Irminger Current (NIIC) flowing northward through Denmark Strait is the main source of salt and heat to the north Iceland shelf. We quantify its along-stream evolution using the first high-resolution hydrographic/velocity survey north of Iceland that spans the entire shelf, along with historical hydrographic measurements as well as data from satellites and surface drifters. The NIIC generally follows the shelf break. Portions of the flow recirculate near Denmark Strait and the Kolbeinsey Ridge. The current's volume transport diminishes northeast of Iceland before it merges with the Atlantic Water inflow east of Iceland. The hydrographic properties of the current are modified along its entire pathway, predominantly because of lateral mixing with cold, fresh offshore waters rather than air-sea interaction. Progressing eastward, the NIIC cools and freshens by approximately 0.3 °C and 0.02–0.03 $\mathrm{g\,kg^{-1}}$ per 100 km, respectively, in both summer and winter. Dense-water formation on the shelf is limited, occurring only sporadically in the historical record. The hydrographic properties of this locally formed water match the lighter portion of the North Icelandic Jet (NIJ), which emerges northeast of Iceland and transports dense water toward Denmark Strait. In the region northeast of Iceland, the NIIC is prone to baroclinic instability. Enhanced eddy kinetic energy over the steep slope there suggests a dynamical link between eddies shed by the NIIC and the formation of the NIJ, as previously hypothesized. Thus, while the NIIC rarely supplies the NIJ directly, it may be dynamically important for the overturning circulation in the Nordic Seas.

Plain Language Summary

The North Icelandic Irminger Current (NIIC) impacts the Icelandic climate and ecosystem by transporting salt, heat, and nutrients onto the north Iceland shelf. It also contributes to the large-scale "overturning circulation" whereby warm water flowing northward in the surface layer is cooled, sinks, and returns to the south at depth. We use a multitude of observational data, including the first high-resolution shipboard survey of temperature, salinity, and velocity that spans the entire north Iceland shelf, to study changes in the NIIC's properties and transport along the current's pathway. The NIIC progresses clockwise along the edge of the shelf around north Iceland. It cools and freshens along the way as it mixes with offshore waters from the Iceland Sea. On the shelf, wintertime heat loss to the atmosphere also cools and densifies the water. However, these locally formed dense waters contribute very little to the dense water that participates in the large-scale overturning circulation.

1 Introduction

Warm, saline Atlantic Water flowing northward into the Nordic Seas and the Arctic Ocean constitutes the northern extremity of the upper limb of the Atlantic Meridional Overturning Circulation (AMOC). Extensive heat loss to the atmosphere in the Nordic Seas cools the inflow. The resulting dense water returns southward at depth and passes through gaps in the Greenland-Scotland Ridge into the deep North Atlantic. This water mass transformation is of key importance to the AMOC, which impacts Earth's climate by transporting heat poleward (Chafik & Rossby, 2019; Årthun et al., 2018; Tsubouchi et al., 2021).

The Atlantic Water crosses the Greenland-Scotland Ridge in Denmark Strait, at the eastern and western sides of the Iceland-Faroe Ridge, and in the Faroe-Shetland Channel (Fig. 1; e.g., Helland-Hansen & Nansen, 1909; Østerhus et al., 2019). The inflow branches to the east of Iceland collectively account for most of the Atlantic Water volume transport across the ridge (Østerhus et al., 2019). This warm and saline water progresses northward through the eastern Nordic Seas while releasing heat to the atmosphere (Mauritzen, 1996; Isachsen et al., 2007). The modified Atlantic Water masses recirculating in Fram

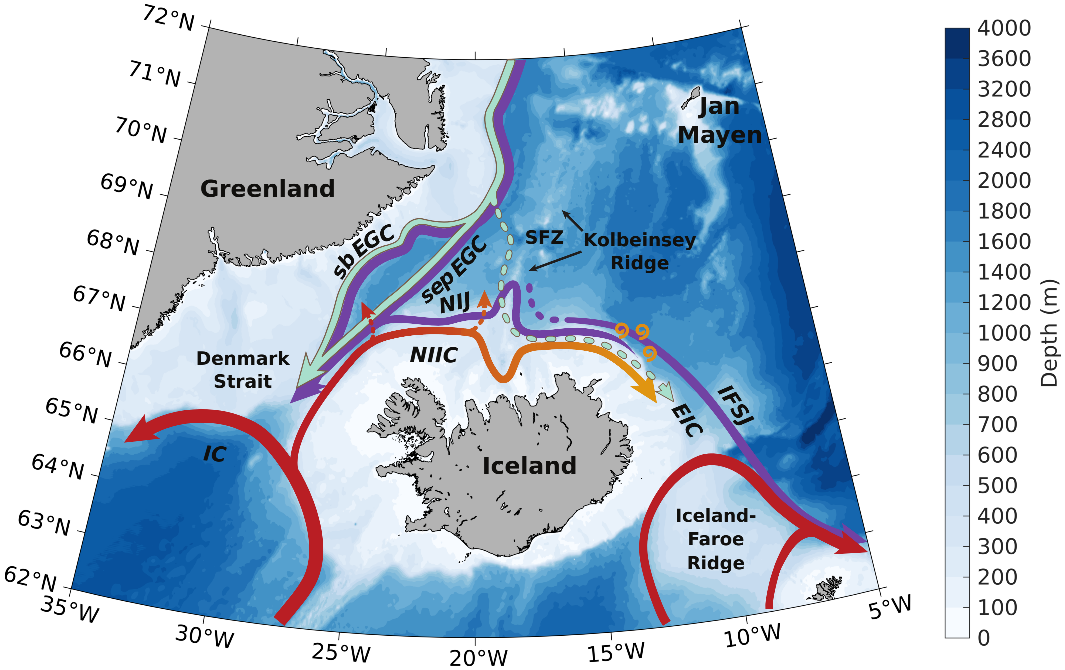

Figure 1. Bathmetry and circulation near the north Iceland shelf. Schematic pathways of the inflow of Atlantic Water into the Nordic Seas (red arrows), the outflow of dense water (purple arrows), and the flow of fresh surface water (light green arrows). The acronyms are: EIC = East Icelandic Current; IC = Irminger Current; IFSJ = Iceland-Faroe Slope Jet; NIIC = North Icelandic Irminger Current; NIJ = North Icelandic Jet; sb EGC = shelfbreak East Greenland Current; sep EGC = separated East Greenland Current; SFZ = Spar Fracture Zone. The colored shading is the bathymetry from ETOPO1 (Amante & Eakins, 2009).

Strait and exiting from the Arctic Ocean merge in the East Greenland Current, which returns the densified water toward the Greenland-Scotland Ridge (Håvik, Pickart, et al., 2017; Rudels et al., 2005). This transformed water is called Atlantic-origin water because of its primary modification in the Atlantic domain in the eastern Nordic Seas (Swift & Aagaard, 1981). The continual along-stream transformation is referred to as the rim current overturning loop.

West of Iceland, the North Icelandic Irminger Current (NIIC) brings Atlantic Water into the Nordic Seas through Denmark Strait. The NIIC bifurcates from the Irminger Current south of the strait and follows the continental slope west of Iceland (Fig. 1). The NIIC has the smallest volume transport of the three inflow branches. Nonetheless, it is a major source of heat, salt, and nutrients to the north Iceland shelf, substantially affecting the local ecosystem (e.g., Jónsson & Valdimarsson, 2012b). The nutrient-rich Atlantic Water facilitates plankton growth on the shelf, which is important for primary production and ultimately the capelin biomass, which in turn is a major food source for the Icelandic cod stock (Stefánsson & Ólafsson, 1991; Thórdardóttir, 1984; Astthorsson & Vilhjálmsson, 2002; Astthorsson et al., 2007). Furthermore, the spawning grounds of some of the main Icelandic fish stocks are located off the island's southwest coast, and their eggs and larvae are transported by the NIIC toward the feeding areas on the northern shelf (Jónsson & Valdimarsson, 2005). The current also impacts the regional climate (e.g., Malmberg & Kristmannsson, 1992). During the so-called "ice-years" between 1965 and 1970, the Atlantic Water inflow to the north Iceland shelf was reduced, and cold, fresh surface water and sea ice covered the shelf (Malmberg & Jónsson, 1997). Since the mid-

1990s, however, the warm Atlantic Water has prevailed on the north Iceland shelf, and the volume, temperature, and salt transports have generally increased (Jónsson & Valdimarsson, 2012b; Casanova-Masjoan et al., 2020).

The path of the NIIC has been investigated in several studies using a variety of methods. Shortly after passing through Denmark Strait, a portion of the NIIC recirculates and returns to the south, as shown from historical hydrographic data (Casanova-Masjoan et al., 2020) and high-resolution numerical simulations (Saberi et al., 2020). While surface drifters indicated that some portion of the NIIC also retroflects when approaching the complex bathymetry west of the Kolbeinsey Ridge (Fig. 1, Valdimarsson & Malmberg, 1999), most of the Atlantic Water continues along the shelf toward northeast Iceland (Jónsson, 2007; Casanova-Masjoan et al., 2020). The presence of the NIIC northeast of Iceland has also been suggested from numerical models (Logemann et al., 2013; Behrens et al., 2017; Zhao et al., 2018; Ypma et al., 2019). However, the ultimate fate of the NIIC remains unclear. The model results of Våge et al. (2011) suggest that the current's volume transport decreases progressing eastward, and what remains of the current may leave the shelf east of Iceland and merge with the Atlantic Water inflow east of Iceland or mix with surface waters from the Iceland and Norwegian Seas and progress eastward (Stefánsson, 1962; Read & Pollard, 1992; Perkins et al., 1998; Ypma et al., 2019). The properties of the NIIC on the shelf east of Iceland may at times be indistinguishable from offshore water masses because of local water mass transformation, making it challenging to trace the NIIC from hydrographic observations alone in this region (Read & Pollard, 1992; Ypma et al., 2019). The fate and pathway of the NIIC may also vary on interannual timescales, as suggested by occasional seaward displacements of the NIIC northeast of Iceland (Macrander et al., 2014) and surface drifters whose trajectories differed between two deployment years (Valdimarsson & Malmberg, 1999).

Northeast of Iceland, the presence of the East Icelandic Current (EIC, Fig. 1) further complicates the picture. There, the EIC merges with the NIIC (Casanova-Masjoan et al., 2020) or, at least at times, continues adjacent to the NIIC (Macrander et al., 2014). The EIC originates from the East Greenland Current and advects cold, fresh surface water and Atlantic-origin water at depth into the Iceland Sea (Jónsson, 2007; Macrander et al., 2014; de Jong et al., 2018). It is still unclear whether this current approaches the Iceland shelf break west of the Kolbeinsey Ridge (Casanova-Masjoan et al., 2020) or east of the ridge after passing through the Spar Fracture Zone (de Jong et al., 2018). East of Iceland, the pathway and velocity of the EIC are variable, as inferred from surface drifters, hydrographic surveys, and moored current meters (Poulain et al., 1996; Perkins et al., 1998). Float trajectories suggest that the EIC progresses from the Iceland Sea into the Norwegian Sea (Voet et al., 2010; de Jong et al., 2018), where its cold, fresh surface waters reduce the ocean heat content and increase the freshwater content (Mork et al., 2019). However, the current's volume transport, extent, and variability remain elusive.

The water transported by the NIIC is modified along its entire pathway. The largest along-stream changes occur west of Iceland during summer and fall when the inflowing Atlantic Water is warmest (Casanova-Masjoan et al., 2020). Polar Water stemming from the southward-flowing East Greenland Current reduces the proportion of Atlantic Water in the NIIC to approximately 68 % prior to reaching the Kolbeinsey Ridge (Jónsson & Valdimarsson, 2005, 2012b). Farther downstream, mixing with the EIC may alter the NIIC's composition further. The NIIC may also be modified by air-sea interaction; the importance of this process relative to along-stream mixing is presently unknown.

During winter, the waters on the shelf are cooled by the atmosphere. Hydrographic observations near Denmark Strait indicate that some of the Atlantic Water can reach densities as high as the overflow water (taken to be denser than $\sigma_\Theta = 27.8\,\mathrm{kg\,m^{-3}}$, Dickson & Brown, 1994). This occurs in particular during winters with strong cooling (Saberi et al., 2020). Numerical simulations suggest that the majority of this overflow water quickly leaves the shelf and recirculates directly southward through Denmark Strait instead of continuing along the north Iceland shelf (Ypma et al., 2019; Saberi et al., 2020).

The overflow water that exits the Nordic Seas through Denmark Strait is mainly composed of the Atlantic-origin water modified in the rim current overturning loop, along with colder, denser water formed in the interior basins of the Greenland and Iceland Seas (Swift & Aagaard, 1981; Strass et al., 1993; Mauritzen, 1996; Mastropole et al., 2017). The latter water mass is referred to as Arctic-origin water (Swift & Aagaard, 1981; Våge et al., 2011) and is primarily advected into Denmark Strait by the North Icelandic Jet (NIJ; Fig. 1; Våge et al., 2011; Harden et al., 2016; Semper et al., 2019). The NIJ follows the continental slope westward, directly adjacent to the eastward-flowing NIIC when the bathymetry steers the two currents into close proximity (Pickart et al., 2017). Northeast of Iceland the eastward-flowing Iceland-Faroe Slope Jet (IFSJ) is located seaward of the NIJ (Fig. 1). This deep current has very similar hydrographic properties to the NIJ and supplies dense water to the Faroe Bank Channel overflow (Semper, Pickart, Våge, Larsen, et al., 2020).

While the origin of the IFSJ is unknown, the NIJ emerges northeast of Iceland (Våge et al., 2011; Semper et al., 2019). Våge et al. (2011) hypothesized that the NIJ is part of an interior overturning loop in the Iceland Sea. According to their idealized numerical simulations, the NIIC and NIJ are dynamically linked through instabilities in the NIIC and water mass transformation in the interior basin. Such instabilities along the front between the NIJ and NIIC have been observed (Huang et al., 2019; Semper et al., 2019; Casanova-Masjoan et al., 2020). This suggests that the NIIC might be instrumental in the emergence of the NIJ.

The unknown fate of the NIIC northeast of Iceland and the undetermined relative importance of air-sea heat fluxes for the modification of the current's properties motivate further investigation of the NIIC and its role in the AMOC. Here we use the first high-resolution hydrographic/velocity survey north of Iceland that spans the entire shelf, in combination with historical hydrographic measurements as well as data from satellites and surface drifters. Based on this collection of observational data sets, we elucidate the pathway and transport of the NIIC, characterize the along-stream evolution of its hydrographic properties, and quantify the water mass transformation on the Iceland shelf and its potential contribution to the Greenland-Scotland Ridge overflows.

2 Data and methods

2.1 Shipboard hydrographic/velocity surveys

Our main data set consists of eight transects from a high-resolution hydrographic/velocity survey conducted on board R/V *Knorr* in September 2011 that crossed the NIIC between Denmark Strait and east of Iceland (Fig. 2). The typical station spacing was 10 km on the shelf, 5–7.5 km in the vicinity of the shelf break, and 5 km over the slope. The hydrographic data were obtained using a Sea-Bird 911+ conductivity-temperature-depth (CTD) instrument. The CTD was mounted on a rosette with Niskin bottles, which were used to collect salt samples for calibrating the conductivity sensor. The final accuracies of the temperature, practical salinity, and pressure are 0.001 °C, 0.002, and 0.3 dbar, respectively (Våge et al., 2011; Semper et al., 2019). We applied the Thermodynamic Equation Of Seawater – 2010 (TEOS-10; IOC et al., 2010) to calculate Conservative Temperature, Θ, and Absolute Salinity, S_A, hereafter referred to as temperature and salinity, respectively.

Upward and downward-facing lowered acoustic Doppler current profiler (LADCP) instruments were mounted on the rosette to measure velocity. The measurements were processed using the LADCP Processing Software Package from the Lamont-Doherty Earth Observatory (Thurnherr, 2010, 2018). The barotropic tides were removed from the ve-

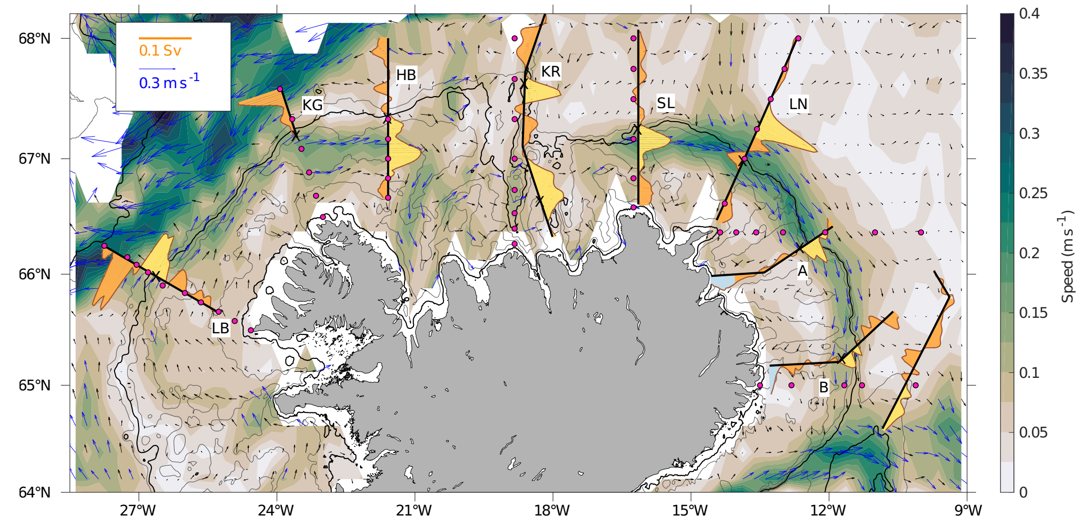

Figure 2. Transects of the high-resolution hydrographic/velocity survey in September 2011 (black lines; see text for station spacing along the transects). At each transect, the shelf break is marked by a black cross. The speed (color) and velocity (black arrows, blue arrows for magnitude $> 0.1\,\mathrm{m\,s^{-1}}$) from surface drifters are shown in the background. The depth-integrated cross-section volume transport in the upper 100 m for each transect is indicated by the shaded curve (yellow segments corresponding to the NIIC; blue segments corresponding to the coastal current; orange segments for the remainder of the transect). The MFRI standard hydrographic stations are shown by magenta circles. The 50 and 400 m isobaths from ETOPO1, which outline the shelf area used for the analyses of the historical hydrographic data, are highlighted in black, while the 100, 200, 300, and 500 m isobaths are contoured in gray. The transect acronyms are: LB = Látrabjarg; KG = Kögur; HB = Hornbanki; KR = Kolbeinsey Ridge; SL = Slétta; LN = Langanes Northeast.

locities using an updated version of a regional inverse tidal model with a resolution of $1/60\,°$ (Egbert & Erofeeva, 2002). See Semper, Pickart, Våge, Larsen, et al. (2020) for details.

We used Laplacian-spline interpolation (Pickart & Smethie, 1998) to construct vertical sections of temperature, salinity, and potential density referenced to the sea surface (hereafter referred to as density), with a grid spacing of 2 km and 10 m. Following Semper et al. (2019), we constructed analogously gridded vertical sections of absolute geostrophic velocity by referencing the integrated geostrophic shear from the hydrographic fields with the depth-averaged LADCP velocity at each grid point. The top and bottom 50 m were excluded from the depth averages for grid points with bottom depths greater than 200 m to avoid undue influence from the surface and bottom boundary layers. The origin of each transect (distance $y = 0$ km) was placed at the shelf break (Fig. 2). The along-stream direction x is taken to be positive toward east, i.e., clockwise direction around Iceland. The distance from the Látrabjarg transect (Denmark Strait) was determined along the midpoints between the 50 m and 400 m isobaths.

The volume transport of the NIIC was estimated from the absolutely referenced geostrophic velocity sections by integrating the positive along-stream velocities in the vicinity of the shelf break (Section 3). In particular, the horizontal boundaries of the NIIC were determined by the distinct bands of the highest positive velocities seen in the vertical sections (Figs. 2 and 6). For each section we also checked that the hydrographic properties associated with this near-shelf break velocity band were consistent with the properties of the same band of the respective upstream and downstream sections. This section-by-section approach considering topography, velocity, and hydrography helped identify the most coherent pathway of the NIIC as captured by our synoptic survey. The Kolbeinsey Ridge section is unique in that there are essentially two shelf breaks (Fig. 6). While some portion of the NIIC follows the outer shelf break, the main flow was located near the coast at the inner shelf break. The hydrographic properties of the latter flow are more similar to the neighboring sections. This branch was therefore considered the main branch for the transport estimate. For all sections, we included only water lighter than $\sigma_\Theta = 27.8\,\mathrm{kg\,m^{-3}}$ (i.e., lighter than overflow water). At Langanes Northeast and Section A, where the current was located seaward of the shelf break, this distinguishes the NIIC from the eastward-flowing IFSJ underneath (Fig. 1).

The uncertainty of the transport estimate combines several error sources. The total error of the LADCP instrument and the processed velocity data was estimated to $3\,\mathrm{cm\,s^{-1}}$, while the inaccuracies in the tidal model are $2\,\mathrm{cm\,s^{-1}}$ north of Iceland (Våge et al., 2011; Semper et al., 2019). The combined uncertainty, determined as the root-sum-square of these two errors, is $3.6\,\mathrm{cm\,s^{-1}}$, which was then scaled by the cross-sectional area of the NIIC at each transect. This is a conservative estimate of the transport error because we do not assume that the errors are uncorrelated across the section. There is also a statistical uncertainty due to the temporal variability of the current, but this cannot be assessed from a single survey.

To further investigate the evolution of the hydrographic properties in the NIIC, measurements from 11 additional hydrographic/velocity surveys were used. These surveys were mainly conducted along the monitoring transects of the Marine and Freshwater Research Institute of Iceland (MFRI, Fig. 2), with increased resolution over the slope. Further details regarding these data sets (Semper et al., 2019; Semper, Pickart, Våge, Torres, & McRaven, 2020a,b; Semper, Våge, et al., 2020), including the R/V *Knorr* 2011 survey, are provided in Semper et al. (2019). For each transect of the 11 surveys, we identified the warm, saline core of the NIIC from the gridded vertical sections of temperature and salinity. Of these grid points, we considered only those with velocity exceeding $0.1\,\mathrm{m\,s^{-1}}$, and divided them into ΘS-classes of $0.1\,°\mathrm{C}$ and $0.005\,\mathrm{g\,kg^{-1}}$. We then determined the envelope of these hydrographic properties, excluding bins containing less than 2 % of the total number of data points. These ΘS-envelopes, which outline the core

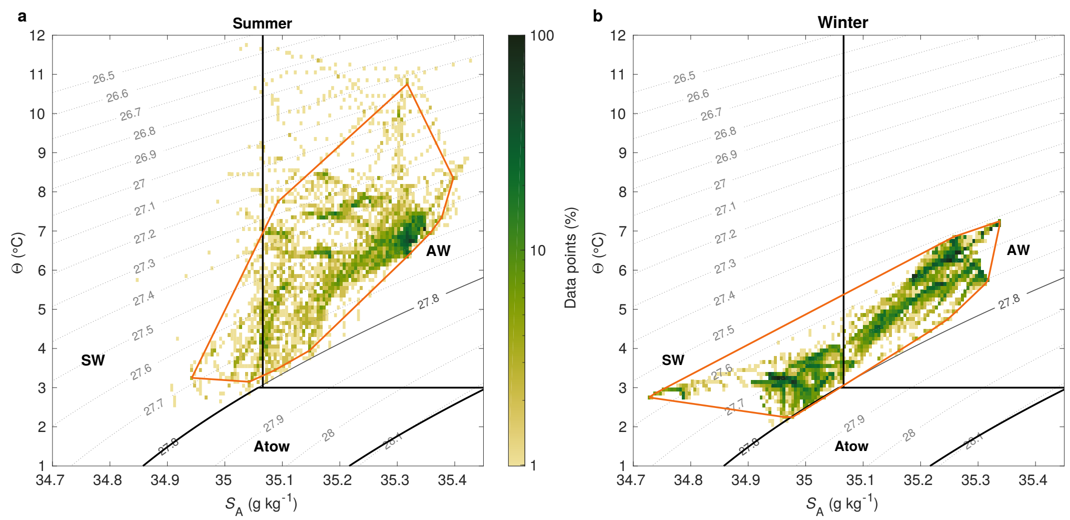

Figure 3. Outline of the NIIC core in ΘS-space. Binned a) summer and b) winter hydrographic properties from all hydrographic/velocity surveys (see text for details). Note the logarithmic color scale. The core of the NIIC is outlined by the envelope (orange polygon), which encompasses all bins that contain at least 2 % of the total number of data points. The gray contours show density. Water masses are separated by thick black lines; their acronyms are: AW = Atlantic Water; Atow = Atlantic-origin water; SW = Surface Water.

of the NIIC, were constructed for summer and winter surveys separately (Fig. 3). As surveys from several years were considered in the analysis, interannual variability in the hydrographic properties of the NIIC is to some extent included in the envelope.

The water masses present in our data are Atlantic Water, which is commonly defined by temperatures and salinities exceeding 3 °C and 35.066 g kg^{-1} (equivalent numbers from Swift & Aagaard, 1981) and overflow water, which is denser than $\sigma_\Theta = 27.8\,\mathrm{kg\,m^{-3}}$ (Dickson & Brown, 1994) but lighter than Nordic Seas Deep Water, which exceeds densities of $\sigma_{0.5} = 30.44\,\mathrm{kg\,m^{-3}}$ (Rudels et al., 2005). The two classes of overflow water, Atlantic-origin and Arctic-origin water, are distinguished by temperatures above and below 0 °C, respectively. The remaining broad range of fresh waters is collectively referred to as Surface Water.

All hydrographic/velocity surveys were used to compute the volume transports of the NIJ and IFSJ in ΘS-space (as in Semper et al., 2019; Semper, Pickart, Våge, Larsen, et al., 2020), which we compare to the composition of dense water on the shelf in Section 6.

2.2 Historical hydrographic measurements

The historical hydrographic observations on the Iceland shelf between 1980 and 2016 used in this study are a subset of the composite data set originally compiled by Våge et al. (2015) and updated by Huang et al. (2020), where information about quality control and the references to the individual data sets are found. The profiles were obtained from the Unified Database for Arctic and Subarctic Hydrography (UDASH), the International Council for the Exploration of the Seas (ICES), the World Ocean Database (WOD), the Argo float program, the Norwegian Iceland Seas Experiment database (NISE), the Global Ocean Data Analysis Project version 2 (GLODAPv2), and the MFRI hydrographic database. We considered only profiles on the Iceland shelf north of Denmark Strait between the 50 and 400 m isobaths to exclude stations near the coast and on the slope, respectively. Duplicate profiles between the different archives were removed from the data set. We refer to winter (summer) profiles as those collected between February and April (July and September). The density at the deepest measurement depth of each profile is taken to represent the bottom density. We determined the mixed-layer depths of the profiles following Våge et al. (2015): Two independent automated routines provided an estimate of the base of the mixed layer, according to a density-difference criterion (Nilsen & Falck, 2006) and the curvature of the temperature profile (Lorbacher et al., 2006). Each hydrographic profile was also visually inspected, and when neither method accurately determined the mixed layer, we manually estimated the mixed-layer depth following the routine used by Pickart et al. (2002).

2.3 Near-surface drifter data

The Global Drifter Program (GDP) is a global 0.25° by 0.25° climatology for measurements from 15-m drogued and undrogued drifters. Version number 3.05 of the climatology includes drifter data collected between February 1979 and April 2019. We used the mean near-surface velocity and its variance. The product is archived and distributed by the Atlantic Oceanographic and Meteorological Laboratory of the National Oceanic and Atmospheric Administration (AOML/NOAA; `https://www.aoml.noaa.gov/phod/gdp/mean_velocity.php`). Documentation of the data set, including details on the corrections applied, is provided by Laurindo et al. (2017).

2.4 Satellite altimetry and sea surface temperature

We used sea level anomalies from the Envisat satellite, which were computed from the difference between the sea surface height and the mean sea surface height of the entire mission at each location. The along-track, filtered sea level anomalies cover the period 2002–2010 at a typical resolution of 7 km. We chose the Envisat mission as it provides the longest continuous record with a repeating orbit to avoid interpolating and smoothing the data. Ground track data points with less than 30 passes or within 30 km of the Iceland coast were removed before the analysis.

Sea surface temperatures were obtained from a reprocessed analysis product based on the Operational SST and Sea Ice Analysis (OSTIA) system. The data are on a global regular grid at 0.05° resolution and provide an estimate of the daily average temperature at 20 cm depth. For consistency, we consider only the time period of the sea surface height anomalies (2002–2010). Both satellite products are distributed by E.U. Copernicus Marine Service Information (`http://marine.copernicus.eu`, product identifiers SEALEVEL_GLO_PHY_L3_REP_OBSERVATIONS_008_062 and SST_GLO_SST_L4_REP_OBSERVATIONS_010_024).

2.5 Atmospheric reanalysis data

To investigate the effect of atmospheric heat fluxes on water mass transformation, we employed the ERA5 atmospheric reanalysis product from the European Centre for Medium-Range Weather Forecasts, which has a spatial resolution of approximately 31 km and a temporal resolution of 1 hour (Hersbach et al., 2020). In particular, we used the surface turbulent heat fluxes and radiation terms on the north Iceland shelf, bounded by the 50 m and 400 m isobaths, from 1980 to 2016.

2.6 Estimation of eddy kinetic energy

Eddy kinetic energy (EKE) was computed from the surface drifter data and the sea level anomalies. In general, EKE can be expressed as

$$\mathrm{EKE} = \frac{1}{2}\left(u'^2 + v'^2\right), \tag{1}$$

where u'^2 and v'^2 are anomalies relative to the mean of the along-stream and cross-stream velocities, respectively. For the altimetry data we make use of the relation between the along-track sea surface height anomalies η' and the cross-track velocity anomalies through geostrophy:

$$u' = \frac{g}{f}\frac{\partial \eta'}{\partial y}, \tag{2}$$

where g is the gravitational acceleration and f is the Coriolis parameter. Since only the surface geostrophic velocity in the cross-track direction can be obtained from along-track altimetry data, isotropy is assumed (Lilly et al., 2003). This implies that the variable parts of the flow in the along-track and cross-track directions have similar amplitudes ($u' \approx v'$), which is a reasonable assumption for an eddy field (von Appen et al., 2016). As such, we simplify Equation 1 for the satellite data to

$$\mathrm{EKE_{sat}} = \frac{1}{2}\left(u'^2 + v'^2\right) \approx u'^2. \tag{3}$$

3 Pathway and transport of the NIIC

The pathway of the NIIC is illustrated by the near-surface flow field inferred from drifters (Fig. 2). The NIIC follows the shelf break northwest of Iceland. Immediately downstream of the Hornbanki section, where the bathymetry becomes complex, the bulk of the NIIC turns southward and flows along the inner shelf break before veering back to the main shelf break as the current approaches the Slétta section. Northeast of Iceland, where the continental slope is steep, the near-surface velocities are particularly enhanced. Prior to crossing the Kolbeinsey Ridge, some portion of the flow is deflected northward (Fig. 2). A retroflection of the NIIC back toward Denmark Strait was identified by Valdimarsson & Malmberg (1999), also using surface drifters. Jónsson & Valdimarsson (2012a) suggested that this recirculation is a semi-permanent feature, as observations from a year-long moored record on the deep western flank of the Kolbeinsey Ridge indicated frequent presence of Atlantic Water in the uppermost 200–300 m. While this off-shelf Atlantic Water may be transported back toward Denmark Strait by the shallow part of the NIJ, which at times extends to the surface (Semper et al., 2019), it may also be entrained into the EIC and advected eastward across the Kolbeinsey Ridge (Jónsson & Valdimarsson, 2012a). The EIC and the NIIC cannot be clearly distinguished in the surface drifter fields, and northeast of Iceland the currents may merge (Fig. 2). South of 65 °N, on the southeast side of Iceland, the remaining flow on the shelf appears to turn eastward and become entrained in the Atlantic Water inflow across the Iceland-Faroe Ridge (Figs. 1 and 2).

The volume transport in the upper 100 m during the 2011 survey is consistent with the velocities inferred from the surface drifter data, indicating that the location of the NIIC during the 2011 survey was similar to the mean configuration of the near-surface flow (Fig. 2). The exception is near the Langanes Northeast transect, where the NIIC was displaced offshore of its climatological location (Fig. 2). Macrander et al. (2014) demonstrated from contemporaneous mooring observations that this seaward displacement lasted several weeks. While such excursions may occur intermittently at this location, the Atlantic Water layer off the shelf was particularly thick during the fall 2011 event (Macrander et al., 2014).

The vertical sections from the 2011 survey show that by the time the NIIC has progressed from Denmark Strait to northeast Iceland, the Atlantic Water, which fills almost the entire shelf, has cooled and freshened substantially (Figs. 4 and 5). We quantify this modification in Section 5. At the most inshore stations of Sections A and B, fresher water with slightly increased velocities is present (Figs. 2, 5, and 6). This is the signature of the anticyclonic coastal current, which is distinct from the NIIC (Valdimarsson & Malmberg, 1999; Astthorsson et al., 2007). Overflow water ($\sigma_\Theta \geq 27.8\,\mathrm{kg\,m^{-3}}$) was observed on the outer shelf at Section B (and at the Hornbanki and Slétta transects, not shown), where the dense water banks up along the slope. This up-tilt of deep isopycnals is a persistent feature along the slope north of Iceland (Semper et al., 2019; Semper, Pickart, Våge, Larsen, et al., 2020). We address the presence of overflow water on the shelf in Section 6.

In the two transects east of Iceland (Sections A and B), a lens of Atlantic Water was located offshore, detached from the core of the NIIC. These lenses divert heat and salt from the shelf into the Iceland Sea, as illustrated by the anticyclonic near-surface eddy in Section B (between 45 and 65 km distance from the shelf break; Figs. 4–6). We investigate the eddy activity northeast of Iceland in Section 4. Formation of eddies is one mechanism that may reduce the transport of the NIIC to some extent (Våge et al., 2011), as the water from the Iceland Sea exchanged during the eddy formation processes will be denser, and any water exceeding the overflow water density limit is not considered in our transport estimate (Section 2).

We now present the volume transport estimates from the September 2011 survey and discuss them in the context of the existing literature. The volume transport of the NIIC generally decreased from west to east (Fig. 7). Between the inflow through Denmark Strait at Látrabjarg and the Hornbanki section 300 km to the northeast, the transport of the NIIC was reduced by approximately 50 %. This decrease likely results from a partial retroflection of the NIIC north of Denmark Strait that has been inferred from numerical simulations (Saberi et al., 2020) and previous transport estimates (Casanova-Masjoan et al., 2020). The retroflection likely accounts for the presence of Atlantic Water on the western side of Denmark Strait (Mastropole et al., 2017).

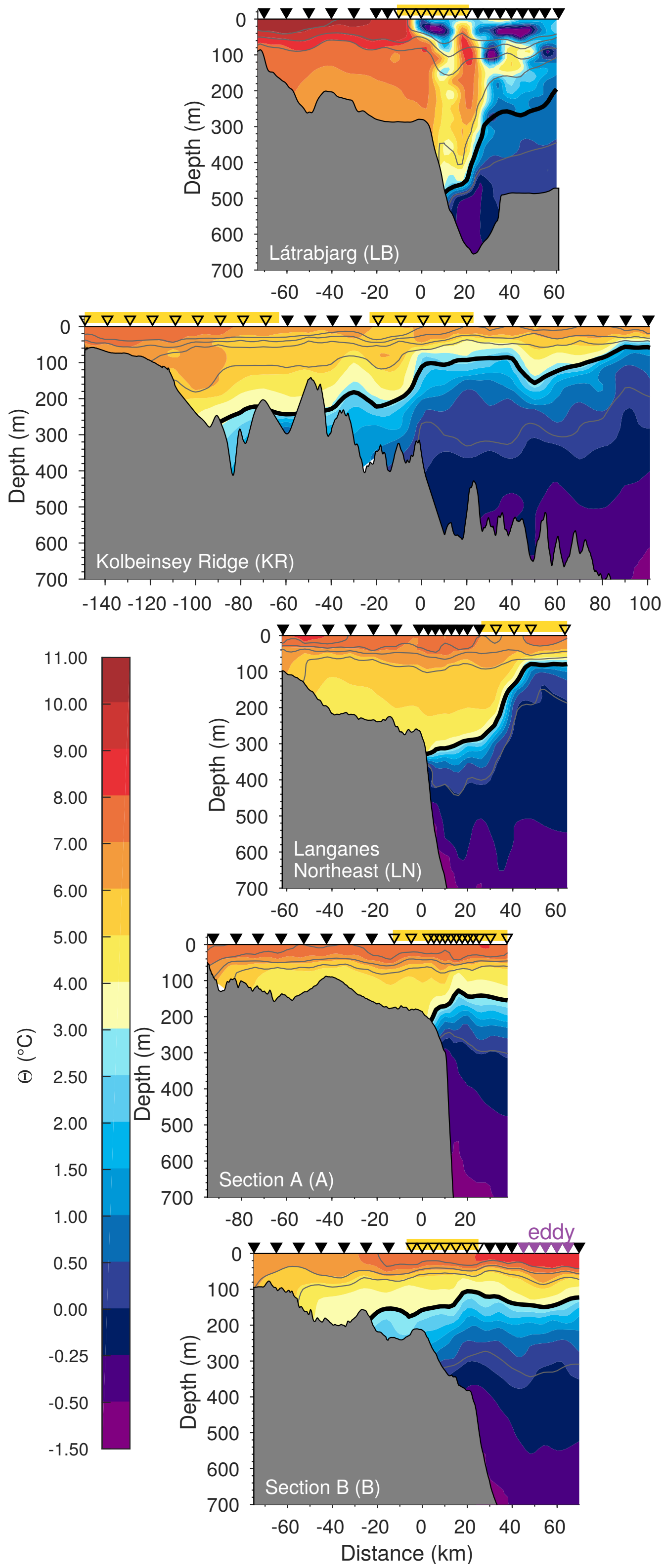

Figure 4. Vertical sections of temperature (color) from the high-resolution hydrographic/velocity survey in 2011 for five transects across the slope north of Iceland (see Fig. 2 for locations). Density is contoured every $0.2\,\mathrm{kg\,m^{-3}}$ (thin gray lines); the $27.8\,\mathrm{kg\,m^{-3}}$ isopycnal is highlighted in black. The black triangles indicate the locations of the stations, and the purple triangles in Section B mark an eddy. Open triangles with a yellow bar mark the segments of each transect used for the transport estimate of the NIIC in the vicinity of the shelf break (the Kolbeinsey Ridge section has an inner shelf break as well (near $-113\,\mathrm{km}$), as discussed in the text). The bathymetry is from the ship's echosounder; the origin of the horizontal axis is placed at the shelf break.

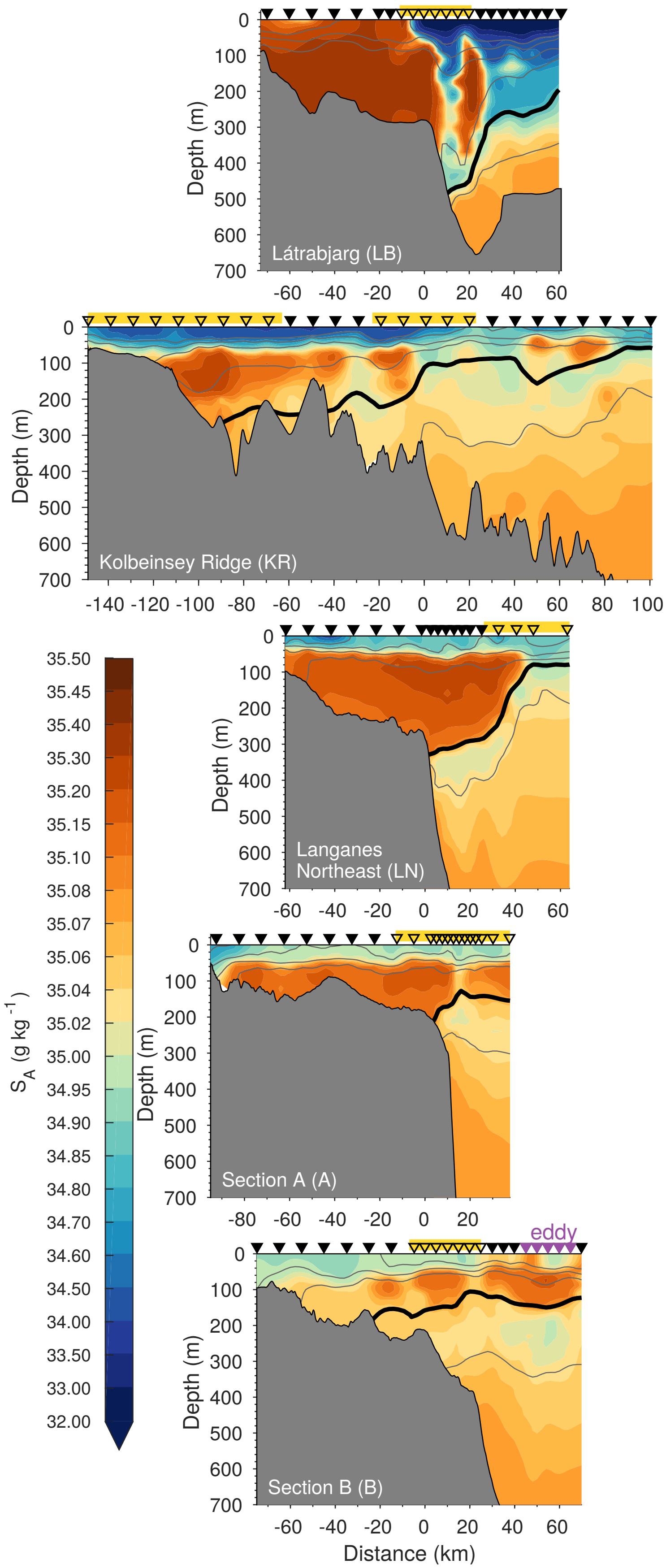

Figure 5. Same as Fig. 4 except for salinity.

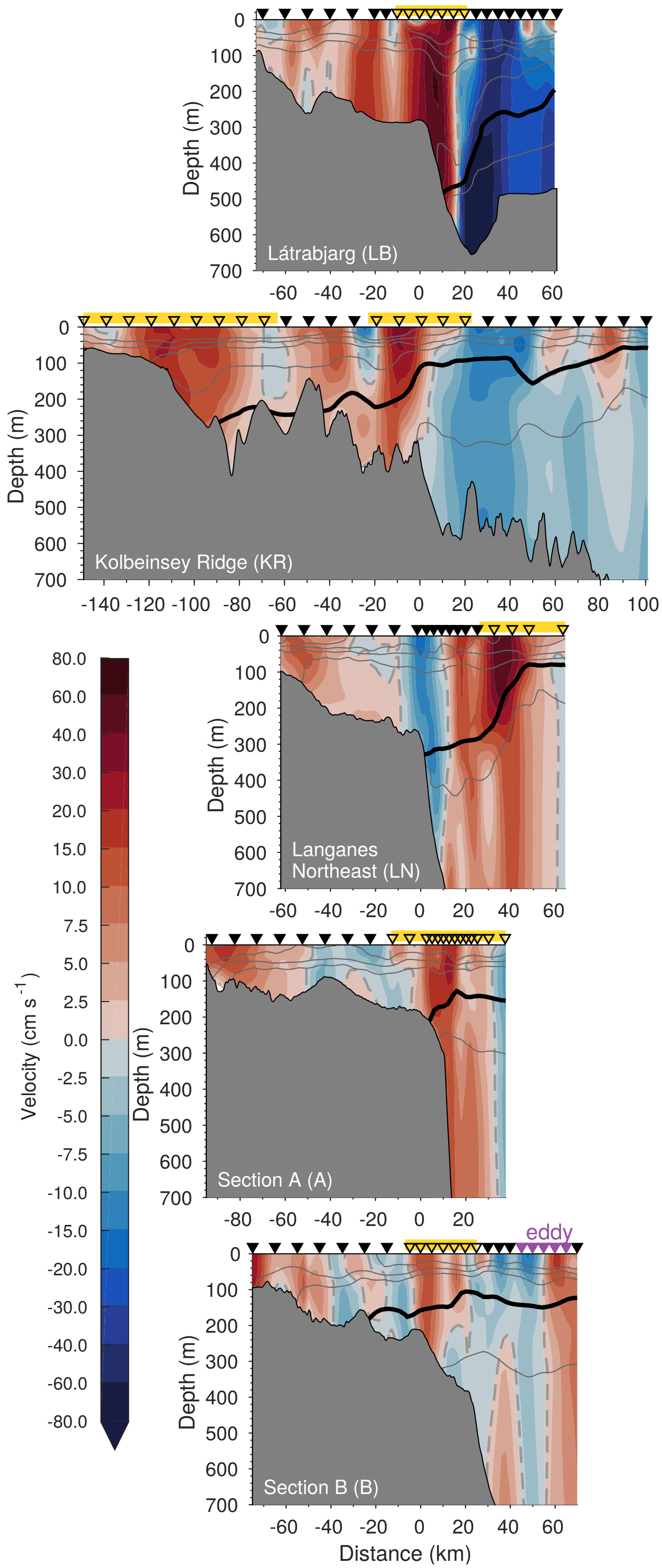

Figure 6. Same as Fig. 4 except for absolute geostrophic velocity (positive velocities are directed clockwise around the island).

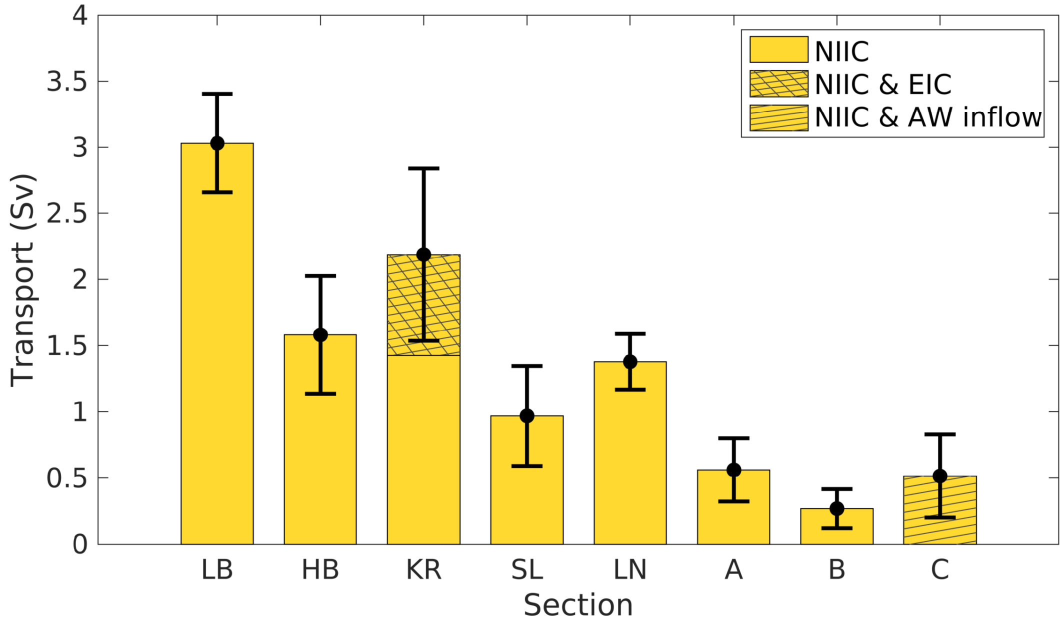

Figure 7. Along-stream volume transport of the NIIC estimated from the high-resolution shipboard survey in 2011. The hatched portions indicate transports where the NIIC has likely merged with the EIC (Section KR) and the Atlantic Water (AW) inflow east of Iceland (Section C). The locations of the sections are shown in Fig. 2. The error bars indicate the uncertainty (see Section 2 for details). The transect acronyms are: LB = Látrabjarg; HB = Hornbanki; KR = Kolbeinsey Ridge; SL = Slétta; LN = Langanes Northeast.

Our transport estimate of $1.6 \pm 0.4\,\mathrm{Sv}$ ($1\,\mathrm{Sv} \equiv 10^6\,\mathrm{m}^3\,\mathrm{s}^{-1}$) for the Hornbanki transect is at the upper end of the range from previous studies. Using 21 years of data from three moorings with limited vertical coverage, the mean Atlantic Water transport of the NIIC at the Hornbanki transect was estimated to $0.9 \pm 0.1\,\mathrm{Sv}$ (Jónsson & Valdimarsson, 2012b; Østerhus et al., 2019). At the nearby Kögur section, which was not sampled in our survey, Pickart et al. (2017) estimated an Atlantic Water transport of $1.71 \pm 0.22\,\mathrm{Sv}$ from six absolute geostrophic velocity sections. Both studies applied an end-member approach distinguishing undiluted Atlantic Water from fresh Polar Water entrained into the NIIC. By contrast, Casanova-Masjoan et al. (2020) investigated the full transport of the NIIC (i.e., not just the Atlantic Water contribution) from gridded satellite altimetry data combined with the MFRI hydrographic sections collected between 1993 and 2017 (typically occupied three to four times per year). They obtained absolute geostrophic velocities using the altimetry data as reference and inferred mean transport estimates for the Kögur and Hornbanki transects of 1.16 ± 0.11 and $1.37 \pm 0.05\,\mathrm{Sv}$, respectively. Our results for the full NIIC transport are based on a single survey, which was conducted in a year with relatively large NIIC volume transports (Casanova-Masjoan et al., 2020). Furthermore, our tight station spacing of approximately 7.5–10 km may have resolved flow that was not captured by the MFRI monitoring stations which are typically spaced 18–20 km apart. Considering the disparate data and methods in addition to the well-documented interannual variability in volume transport of the NIIC (e.g., Jónsson & Valdimarsson, 2012b; Zhao et al., 2018; Casanova-Masjoan et al., 2020), our Hornbanki transport estimate appears reasonable and complements the range of earlier results.

Toward the next section along the Kolbeinsey Ridge the volume transport increased (Fig. 7), likely due to the influence of the EIC. The main portion of the NIIC was found in the vicinity of the inner shelf break at the Kolbeinsey Ridge section (Fig. 6). This velocity core bracketed the warmest and saltiest Atlantic Water signature. Farther offshore, the second velocity core had a weaker lens of Atlantic Water, but immediately above this was a region of slightly colder water with surface-intensified velocities (Figs. 4 – 6) indicative of the EIC. As the EIC most likely constitutes a significant fraction of the outer core (whose portion of the Kolbeinsey Ridge transport is hatched in Fig. 7), the total Kolbeinsey Ridge transport value is anomalously large. This double-core structure is consistent with the mean hydrographic and velocity sections of Casanova-Masjoan et al. (2020). The MFRI standard section closest to the Kolbeinsey Ridge is the Siglunes line (roughly 20 km to the west), and the long-term mean of this section displays two velocity cores at nearly the same locations as the two cores in Fig. 6. Casanova-Masjoan et al. (2020) identified the inner core as the NIIC and the outer core as the EIC since it contained only a small percentage of their Atlantic Water end member. The fate of this outer velocity core remains an open question. The mean sections of Casanova-Masjoan et al. (2020) indicate that the EIC and the NIIC merge. While the horizontal resolution of these sections is relatively low, we cannot exclude a minor contribution from the EIC in our transport estimates farther east. However, according to Macrander et al. (2014), the EIC did not merge with the core of the NIIC in fall 2011 (around the time of our survey) but flowed farther offshore.

Progressing farther eastward, the next significant change in volume transport occurs between Langanes Northeast and Section A (Fig. 7). This reduction in volume transport of the NIIC could be caused by a portion of the flow branching off the main flow, although it should be kept in mind that temporal variability may affect the changes in transport between all consecutive sections in the survey. This off-branching flow could be a recirculation or an offshore branch at Section A (where our section does not extend as far beyond the shelf break as at Langanes Northeast). The lower transport at Section A could also be the result of locally enhanced eddy activity, which is addressed below in Section 4. Note that we excluded the observed eddy at Section B from the NIIC transport. Finally, the volume transport increase at Section C, east of Iceland (Fig. 7), can be explained by the Atlantic Water inflow from the south merging with the remnant of the NIIC (Fig. 2). This is corroborated by the presence of warmer and more saline water compared to the upstream sections (we have therefore hatched the Section C transport value in Fig. 7).

4 Eddy activity northeast of Iceland

Northeast of Iceland the continental slope steepens and velocities are enhanced (Fig. 2). Furthermore, troughs that bisect the shelf are common in this region (Fig. 2). As locally steep topography generally tends to make currents more baroclinically unstable (e.g., Spall, 2010), the NIIC may be particularly susceptible to baroclinic instability northeast of Iceland. Likewise, topographic irregularities such as troughs favor both baroclinic and barotropic instability by changing the potential vorticity of the flow (Chérubin et al., 2000).

The NIIC is likely subject only to baroclinic instability, not barotropic instability (Casanova-Masjoan et al., 2020). To investigate the latter, we expanded the analysis of Casanova-Masjoan et al. (2020) using our September 2011 hydrographic/velocity data. Relative to their sections, our data set has a higher horizontal resolution that better reveals extrema in the lateral gradient of the along-stream velocity. Nonetheless, we found that the necessary condition for barotropic instability is not fulfilled in the NIIC (not shown), in agreement with Casanova-Masjoan et al. (2020). By contrast, the current generally satisfies the necessary condition for baroclinic instability (Casanova-Masjoan et al., 2020).

If the NIIC is baroclinically unstable northeast of Iceland, eddies may form that detach from the current and divert heat and salt off the Iceland shelf. The 2011 Langanes Northeast transect (Figs. 2 and 6) reveals that the NIIC had deviated from its climatological mean position, indicative of an unstable, meandering current (Corlett & Pickart, 2017). At Section B a detached eddy was observed, whose temperature and salinity match the water in the NIIC (Figs. 4–6).

To investigate whether eddy formation is partly responsible for the drop in NIIC volume transport between Langanes Northeast and Section A (Fig. 7), we computed the mean EKE both from along-track satellite altimetry and surface drifters (Section 2) north and east of Iceland. We excluded the western Iceland Sea where the high EKE in the East Greenland Current resulting from substantial mesoscale variability in the vicinity of Denmark Strait (e.g., Håvik, Våge, et al., 2017) overwhelms the signals farther east. Notably, the area between Langanes Northeast and Section A corresponds to a local maximum in EKE, which is apparent from both data sets (Fig. 8a and b). This suggests that eddies are common features in this area. The eddy observed at Section B was thus likely formed farther upstream and advected eastward by the EIC.

The EKE over the slope far exceeds the EKE within the Iceland Sea gyre, which we take to be the background level EKE (Fig. 9). The gyre has been identified by the dynamic height of the sea surface (Våge et al., 2013); its southwestern part is located seaward of the box indicated in Fig. 8. Compared to the gyre, the seasonal variability is more pronounced over the steep continental slope: the eddy activity is particularly enhanced between November and January, while it is significantly lower in early summer (Fig. 9). The strong wintertime EKE signal is reflected in the pronounced variability in sea surface temperature in the same area (Fig. 8c). By contrast, the temperature front between the NIIC and the surface waters farther offshore is weakened during summer (not shown), likely due to the presence of a warm, fresh surface layer that extends from the shelf into the interior Iceland Sea (Pickart et al., 2017; Semper et al., 2019) and that may mask the surface signature of the eddies.

While our results cannot conclusively demonstrate a link between the steep slope northeast of Iceland, a baroclinically unstable NIIC, and the formation of eddies, comparison to better-studied areas is instructive. This can elucidate the implications of the eddy activity for the Iceland Sea. Localized eddy formation due to unstable boundary currents over steep topography is common, for example in the Lofoten Basin (Isachsen et al., 2012; Richards & Straneo, 2015) and the Labrador Sea (Lilly et al., 2003; Gelderloos et al., 2011), where the lateral heat fluxes from these eddies play an important role for the water mass transformation. In the Labrador Sea, anticyclonic warm-core eddies with radii of 15–30 km detach from the West Greenland Current, and EKE is particularly enhanced during winter (Lilly et al., 2003; Pacini & Pickart, 2022). The size of these so-called Irminger Rings is determined by the length scale over which the slope changes in the along-stream direction (Bracco et al., 2008). The size inferred from the topographic length scale northeast of Iceland is consistent with the smaller radius of approximately 10 km for the anticyclonic eddy identified in our high-resolution survey.

Such interplay between boundary currents and the interior basin has also been suggested for the Iceland Sea. In particular, Pickart et al. (2017) proposed that the dynamics of the NIIC and the NIJ may be linked through the locally enhanced exchange of heat and salt from the NIIC to the interior Iceland Sea by eddies. Our results identify the slope northeast of Iceland as locus of the eddy activity. The observations of enhanced eddy kinetic energy presented here are also consistent with the idealized numerical simulations of Våge et al. (2011). According to their study, the NIIC sheds eddies into the interior basin, where the warm water is transformed by air-sea heat exchange. The densified water subsequently returns to the continental slope and sinks, supplying the NIJ. A high-resolution numerical simulation also identified the boundary current system north of Iceland and water mass transformation in the Iceland Sea as key to the formation of the NIJ (Behrens et al., 2017). However, wintertime observations demonstrate that the product of local water mass transformation in the Iceland Sea is not sufficiently dense to ac-

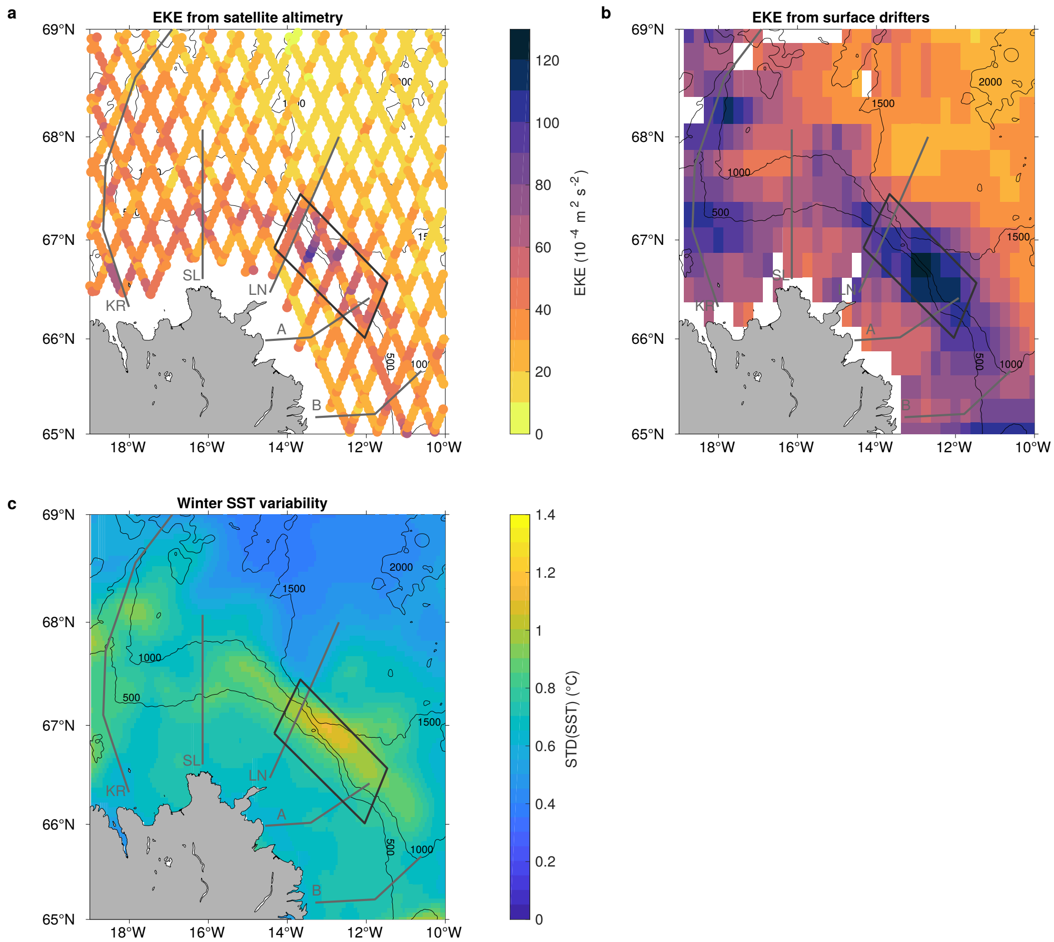

Figure 8. Mean EKE northeast of Iceland inferred from a) along-track satellite altimetry (Envisat) in the period 2002–2010, and b) surface drifter velocities. c) Standard deviation of sea surface temperature obtained from the OSTIA product for January to March 2002–2010. The region of enhanced eddy activity is highlighted in black in each panel. The transects from the high-resolution hydrographic/velocity survey in 2011 are marked in gray. The 500, 1000, 1500, and 2000 m isobaths from ETOPO1 are contoured. The transect acronyms are: KR = Kolbeinsey Ridge; SL = Slétta; LN = Langanes Northeast.

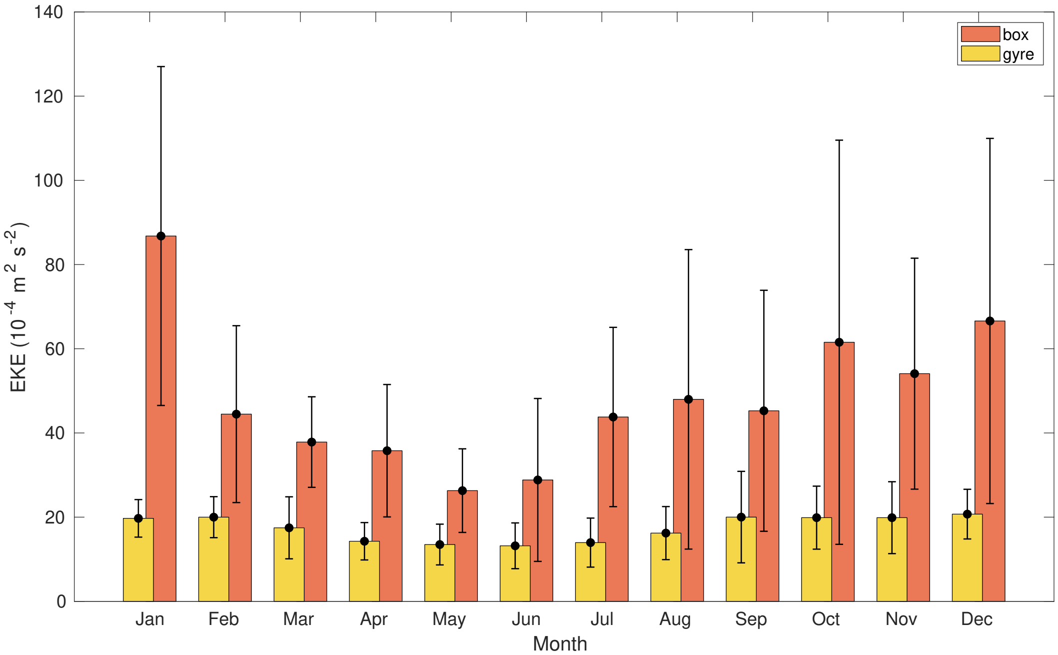

Figure 9. Seasonality of EKE northeast of Iceland. Monthly mean EKE within the Iceland Sea gyre as defined by the dynamic height contours of the sea surface (Våge et al., 2013, yellow bars) and the box in Fig. 8 delimiting the area of enhanced eddy activity northeast of Iceland (orange bars). The EKE has been inferred from along-track satellite altimetry over the period 2002–2010. The error bars indicate the standard deviation.

count for the bulk of the NIJ (and the IFSJ) in the present climate (Våge et al., 2015, in revision). Tracing the Atlantic Water in the NIIC in two ocean circulation models, Ypma et al. (2019) also showed that very little of this water ultimately supplies the overflow through Denmark Strait. Finally, the Greenland Sea has recently been identified as the main source of dense water to the NIJ (Semper et al., 2019; Huang et al., 2020). All of this suggests that the NIIC plays only a marginal role as a source of water to the NIJ. However, it is still unclear how the dense water from the Greenland Sea is entrained into the NIJ and how and why the current first emerges northeast of Iceland (Semper et al., 2019). As this region also has a local EKE maximum, a dynamical aspect of the link between the NIIC and the NIJ, as hypothesized by Våge et al. (2011) and consistent with the implications of our results, may still hold.

5 Along-stream evolution of the NIIC

The vertical sections from the 2011 survey (Figs. 4–6) demonstrate that the hydrographic properties in the NIIC evolve substantially from Denmark Strait to east of Iceland. We investigate this further using all available hydrographic measurements on the north Iceland shelf collected during summer and winter (Section 2), acknowledging the fact that there is an advective time scale of 2–3 months from west to east. For each profile, we averaged the hydrographic properties that fall within the corresponding envelope of the NIIC core (Fig. 3).

The distribution of these mean hydrographic properties (Fig. 10) shows a general tendency of cooling and freshening with increasing distance from Denmark Strait in summer and winter. The inflow of Atlantic Water through Denmark Strait is warmer in sum-

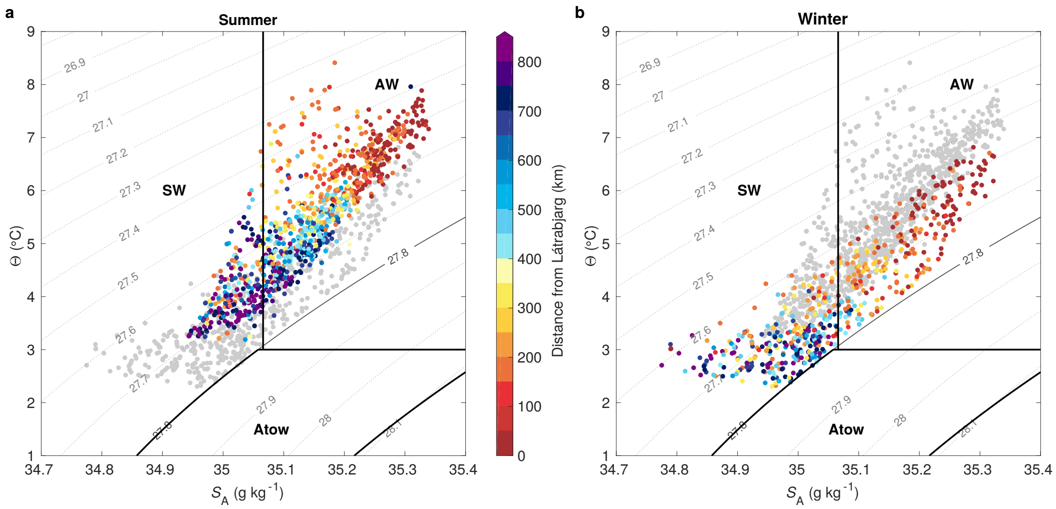

Figure 10. Distribution of hydrographic properties in the NIIC. ΘS-diagram of a) summer and b) winter hydrographic properties in the NIIC from the historical measurements. The mean of each profile within the core of the NIIC as defined from hydrographic/velocity surveys (see Section 2 for details) is colored by distance from the Látrabjarg transect (Denmark Strait). For reference, the properties of winter and summer are shown by gray dots in the background in panels a) and b), respectively. The gray contours are density. The water masses are separated by thick black lines; their acronyms are: AW = Atlantic Water; Atow = Atlantic-origin water; SW = Surface Water.

mer than in winter, which agrees with previous studies (e.g., Casanova-Masjoan et al., 2020; Jónsson & Valdimarsson, 2012b).

In winter the NIIC is generally colder, and the fresh water mass classified as Surface Water dominates most of the stations beyond the Kolbeinsey Ridge (approximately 450 km northeast of Denmark Strait). This water, resulting from wintertime transformation on the shelf, is also known as North Icelandic Winter Water (Stefánsson, 1962). It may mix with ambient denser waters in the Iceland and Norwegian Seas and eventually contribute to the overflows across the Iceland-Faroe Ridge and possibly the Faroe Bank Channel (Meincke, 1974; Read & Pollard, 1992; Hansen & Østerhus, 2000; Fogelqvist et al., 2003; Ypma et al., 2019).

The winter properties are mainly confined between the 27.6 and 27.8 $\mathrm{kg\,m^{-3}}$ isopycnals. We emphasize that these winter hydrographic properties are found within the core of the NIIC, and that denser waters can be present on the shelf as observed at several transects in the 2011 survey (Section 3). A few of the profiles near Denmark Strait are as cold, fresh, and dense as some of the easternmost profiles. These waters may have been advected by the NIIC through Denmark Strait or were formed locally on the shelf. Such local water mass transformation is explored in Section 6.

To quantify the along-stream evolution of the NIIC, we grouped the hydrographic properties from Fig. 10 according to distance from Denmark Strait. We chose the distance classes such that each class contained one of the MFRI monitoring sections, ensuring an adequate number of profiles in each group (Fig. 11e and f). In summer, the NIIC cools from $6.7 \pm 0.4\,°\mathrm{C}$ at Látrabjarg to $4.2 \pm 0.5\,°\mathrm{C}$ east of Iceland and freshens from $35.25 \pm 0.03\,\mathrm{g\,kg^{-1}}$ to $35.05 \pm 0.04\,\mathrm{g\,kg^{-1}}$, where the uncertainties are the difference between the median and the 25th or the 75th percentile (whichever was larger). This corresponds to a reduction in temperature and salinity of 0.3 °C and 0.02 g kg^{-1} per 100 km, respectively (Fig. 11a and b). During winter, the inflow at Látrabjarg is approximately 1.1 °C colder than in summer. During this season the NIIC cools from 5.6 ± 0.9 °C to 2.9 ± 0.2 °C and freshens from 35.23 ± 0.06 g kg^{-1} to 34.95 ± 0.06 g kg^{-1} toward east Iceland. The winter trends for the decrease in temperature and salinity are 0.3 °C and 0.03 g kg^{-1} per 100 km, respectively. The 25th percentiles of the summer salinity overlap with the 75th percentiles of the winter salinity on the western shelf, indicating that the inflow's seasonal change in salinity is less pronounced than in temperature. All trends are significant at the 99 % confidence level according to the Student's t test.

Most of the transformation during winter occurs west of the Kolbeinsey Ridge (approximately 450 km northeast of Denmark Strait). This is consistent with the findings of Casanova-Masjoan et al. (2020), who argued that the hydrographic properties of the NIIC are primarily modified before it merges with the EIC. However, the two sets of results cannot be quantitatively compared because we considered the along-stream evolution of the NIIC core, whereas Casanova-Masjoan et al. (2020) referred to the merged flow of the EIC and NIIC and applied a static Atlantic Water definition of warmer than 3 °C.

While the cooling and freshening rates of the NIIC are not significantly different in summer and winter (0.3 °C and 0.02–0.03 g kg^{-1} per 100 km, quantified by a regression analysis), the increase in density is significantly different at the 95 % confidence level between the seasons. The NIIC cools slightly more and freshens slightly less in summer, both of which increases the density relative to the winter scenario. This is reflected in the evolution of the median density over distance and in ΘS-space (Fig. 11c and d). The transformation during summer is less isopycnal than during winter, when density changes due to freshening and cooling approximately balance. This suggests that atmospheric heat loss plays only a minor role in cooling the core of the NIIC in winter. (In summer, the net atmospheric heat flux changes sign and the ocean gains heat.) Instead, isopycnal mixing with cold, fresh surrounding waters is the dominant process responsible for the modification of the NIIC. As the cooling and freshening signal is larger on the outer shelf than near the coast (not shown), the water mixing with the NIIC must originate from offshore, in the Iceland Sea.

To support the notion that atmospheric heat loss plays a minor role in modifying the core of the NIIC, we carried out the following simple calculation. First we estimated the wintertime heat loss between our survey lines using the NIIC temperatures from the historical hydrographic data set (Fig. 11). Then, for an idealized water column of 200 m depth and 1 m^2 in surface area, we integrated atmospheric heat fluxes from ERA5 over the respective area for the period of the travel time inferred from the NIIC's velocity. The observed cooling between two survey lines from Fig. 11, minus that due to the air-sea heat flux, is the cooling due to other processes such as mixing with colder water masses. Our rough estimates indicate that atmospheric heat loss contributes as little as 5–25 % to the wintertime modification of the NIIC core along the north Iceland shelf.

6 Water mass transformation on the north Iceland shelf

The considerable along-stream modification of the NIIC motivates us to investigate the water mass transformation of all waters on the north Iceland shelf in more detail. While overflow water is commonly present on the shelf, it is unclear whether this results from advection or local formation. We now assess the local formation of overflow water on the shelf and possible contributions to the NIJ and IFSJ. As in Section 5, we consider the historical hydrographic data north of Denmark Strait.

The mean mixed-layer density on the north Iceland shelf in winter is 27.7 kg m^{-3} with a standard deviation of 0.1 kg m^{-3}. Of the 806 winter profiles, 85 (11 %) have mixed

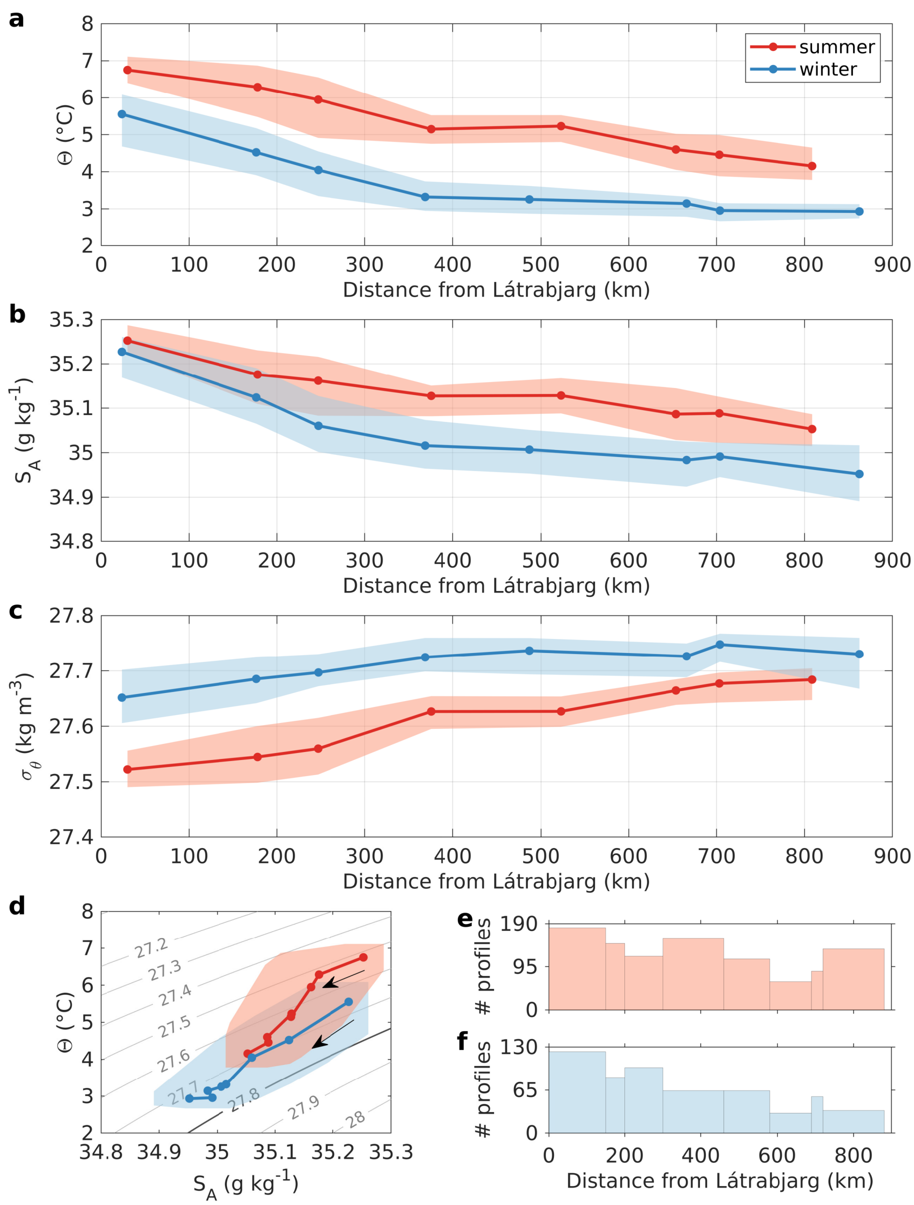

Figure 11. Along-stream evolution of a) temperature, b) salinity, and c) density in the core of the NIIC for summer (red) and winter (blue) from the historical hydrographic measurements in Fig. 10. The median properties of each distance class are marked at their mean distance from the Látrabjarg transect (Denmark Strait). The range between the 25th and 75th percentiles is indicated by the shading. The evolution of the median properties in ΘS-space is shown in d), where the area between the 25th and 75th percentiles is covered by the envelope. The arrows point toward increasing distance from Látrabjarg. The number of profiles per distance class for summer and winter is displayed in panels e) and f), respectively (note the different scales on the y-axis).

layers that exceed overflow water density (Fig. 12a). (Unsurprisingly, none of the 1197 summer profiles has such a dense mixed layer.) However, dense winter mixed-layers do not necessarily imply significant local overturning, as less than one-third of these profiles are homogeneous all the way to the bottom (Fig. 12a). Of all winter profiles, less than 3 % are both homogeneous to the bottom and exceed the density of overflow water.

We note that the vast majority (85 %) of the winter profiles were obtained in February, and further heat loss likely continues to densify the mixed layers until the end of winter. To estimate the mean mixed-layer density at the end of April, we used a one-dimensional mixed-layer model known as the PWP-model (Price et al., 1986), which has previously been employed in the Iceland Sea (e.g., Moore et al., 2015; Våge et al., 2018). We initialized the model with the average temperature and salinity profiles from all of the February measurements (where the bottom depth of the mean profile is 400 m and the initial mixed-layer depth is approximately 150 m). The mean winter heat fluxes from ERA5 on the north Iceland shelf over the sampling period 1980–2016 were imposed at the surface at each time step. We applied the forcing over three months (February–April), conservatively assuming that all February profiles – irrespective of their sampling date – were exposed to cooling for the entire period. The simulations indicate that only by increasing the atmospheric forcing by 50 % above the mean ERA5 values, does the mean mixed layer attain overflow water density. While mixed-layer densities exceeding 27.8 $\mathrm{kg\,m^{-3}}$ may have occurred more often than the historical hydrographic data set biased toward February suggests, an additional three months of heat loss for the most part did not result in overflow water formation by the end of the winter season.

The bottom densities on the shelf greatly exceed the mixed-layer densities (Fig. 12b). Overflow water occupies the deepest part of the water column, in particular where troughs bisect the shelf, such as north (near 19 °W) and east (near 66 °N) of Iceland. We identified a total of 739 profiles with overflow water at depth. The large majority of these profiles were stably stratified; only 24 profiles were vertically homogeneous. This suggests that there are two distinct causes for the presence of overflow water on the shelf: local transformation of the mixed layer and the up-banking of dense water near the shelf break at depth, with the latter being the dominant cause. This is consistent with the fact that the dense water at depth is present both in summer and winter (Fig. 12b), and agrees with the results of Jochumsen et al. (2016), who demonstrated that there is no significant seasonal variability of the bottom temperature and salinity properties below approximately 250 m depth on the Iceland shelf. In the 2011 survey, overflow water was observed near the shelf break at several transects (Section 3). Such up-banking of dense water along the north Iceland slope supports the middepth-intensified structure of the NIJ, and is well documented (Jónsson & Valdimarsson, 2004; Våge et al., 2011; de Jong et al., 2018; Semper et al., 2019). The mechanism causing the up-banking of the dense water remains to be studied.

The occurrence of dense mixed layers, however, can likely be explained by local water mass transformation (Fig. 12a). Before the mid-1990s, dense-water formation on the north Iceland shelf appeared to be more common, whereas mixed layers denser than $\sigma_\theta = 27.8\,\mathrm{kg\,m^{-3}}$ have scarcely been observed since (Fig. 12c). This agrees with the notion that the waters on the shelf have become warmer and saltier over the past decades (Casanova-Masjoan et al., 2020), with the net effect of a slightly decreasing trend in density. However, considering that the majority of the wintertime profiles stem from after 1995, conclusions regarding dense-water formation on the shelf before 1995 are tentative. After the mid-1990s, there were only three winters (1995, 2004, and 2016) when more than one-third of the mixed layers on the shelf exceeded overflow water density. Geographically, these dense profiles were observed over a large area on the central northern shelf. This suggests that the dense mixed layers result from transformation on the northern shelf, downstream of the inflow through Denmark Strait.

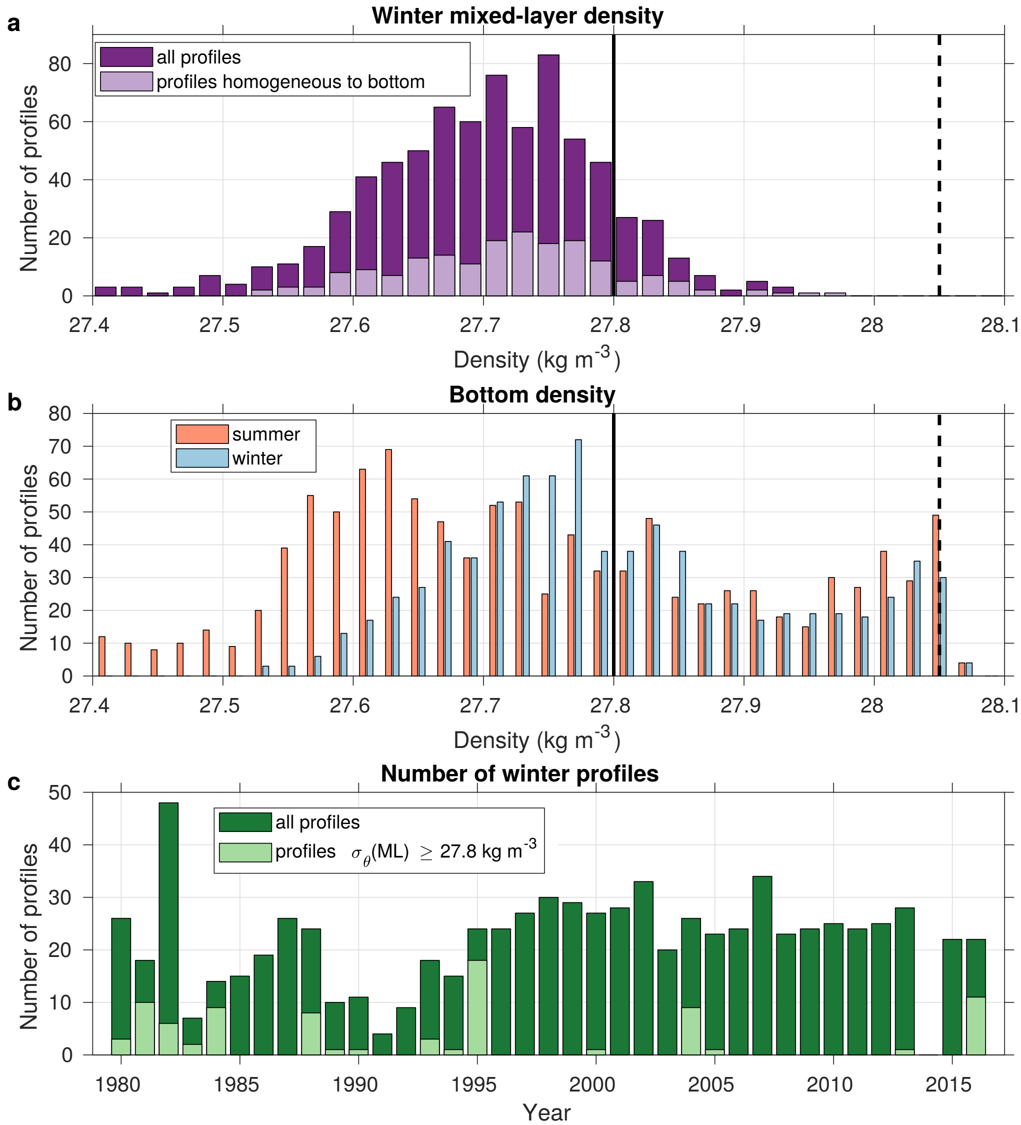

Figure 12. Density distribution and number of winter profiles per year on the north Iceland shelf. Distribution of a) mixed-layer density for all winter profiles (purple), including the subset of profiles that are homogeneous all the way to the bottom (light purple); and b) bottom density for all summer (red) and winter (blue) profiles. The x-axis is truncated at $27.4\,\mathrm{kg\,m^{-3}}$ for increased legibility. The $27.8\,\mathrm{kg\,m^{-3}}$ isopycnal delimiting overflow water and the $28.05\,\mathrm{kg\,m^{-3}}$ isopycnal indicating the transport mode of the NIJ (Semper et al., 2019) are marked by the solid and dashed black lines, respectively. c) Interannual variability in the number of winter profiles (green), including the subset of profiles with mixed layers (ML) exceeding the density of overflow water (light green).

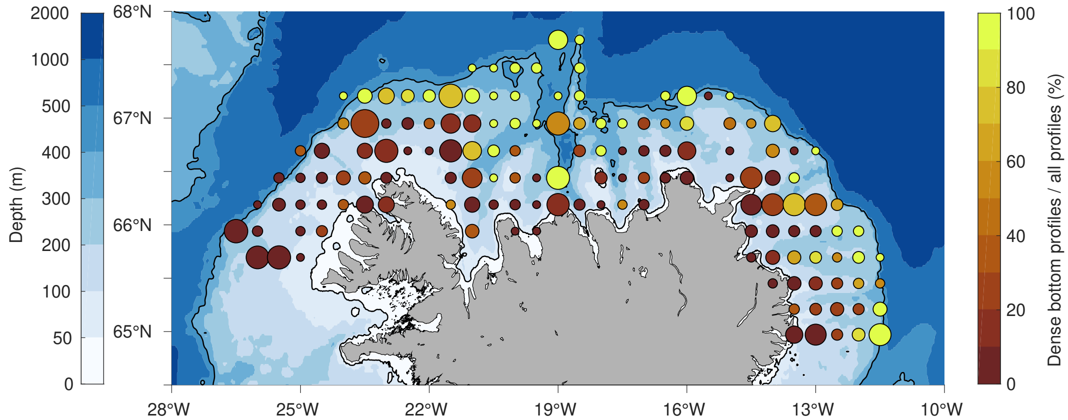

Figure 13. Map showing the ratio of profiles (from all seasons) with bottom densities exceeding overflow water density to the total number of profiles located within 0.5° longitude $\times$ 0.25° latitude bins. Due to the binning, the locations of some of the markers extend outside the 50 and 400 m isobaths highlighted in black. The number of total profiles per bin, ranging from 1 to 157, is proportional to the size of the markers. The colored shading is the bathymetry from ETOPO1.

Interestingly, the hydrographic properties of the overflow water on the shelf differed considerably between these three years: the mixed layers were warm and saline in 2004 and 2016, but cold and mostly fresher in 1995 (Fig. 14). The mixed-layer properties of all years partly match the hydrographic properties of the upper layers of the NIJ, and to some extent the IFSJ (the IFSJ observations are based on a single survey, Semper, Pickart, Våge, Larsen, et al., 2020). The upper portion of the currents (which is more variable in properties than the deeper portion), contains Atlantic-origin water. As such, water mass transformation on the north Iceland shelf may, on rare occasions, contribute to this component of the Denmark Strait and Faroe Bank Channel overflows. We note, however, that it is unclear to what extent waters from the north Iceland shelf may be entrained into the IFSJ, which is located farther offshore than the NIJ (Semper, Pickart, Våge, Larsen, et al., 2020). Considering that the NIJ often shares a common front with the NIIC (Pickart et al., 2017), and that there may be a dynamical link between these two currents (Section 4; Våge et al., 2011), direct entrainment of dense shelf waters is more likely for the NIJ than for the IFSJ. In any case, Arctic-origin overflow water accounts for a more substantial volume transport in both the NIJ and the IFSJ, and such dense water was not observed in the mixed layers on the north Iceland shelf. This is consistent with previous observational studies suggesting a Greenland Sea origin for the densest portion of these currents (Pickart et al., 2017; Brakstad et al., 2019; Semper, Pickart, Våge, Larsen, et al., 2020; Huang et al., 2020).

The recent numerical simulations by Garcia-Quintana et al. (2021), who argued that the Iceland shelf is an important source of water to the NIJ, are not consistent with our results. Their modeling study suggests that wintertime water mass transformation on the northwestern Iceland shelf leads to the formation of overflow water and dense-water plumes that supply up to 20 % of the NIJ's volume transport. The model's density structure is not representative of the observations, in particular near the coast, where the stratified, fresh coastal current is present. In this region, dense mixed layers extending to the bottom form in the model and supply the dense-water plumes that cascade through the submarine canyons north of Iceland. This is incongruent with the observations. Furthermore, the high salinity of the overflow water that supplies the NIJ in the model, resulting from direct transformation of the saline Atlantic Water in the NIIC, is not consis-

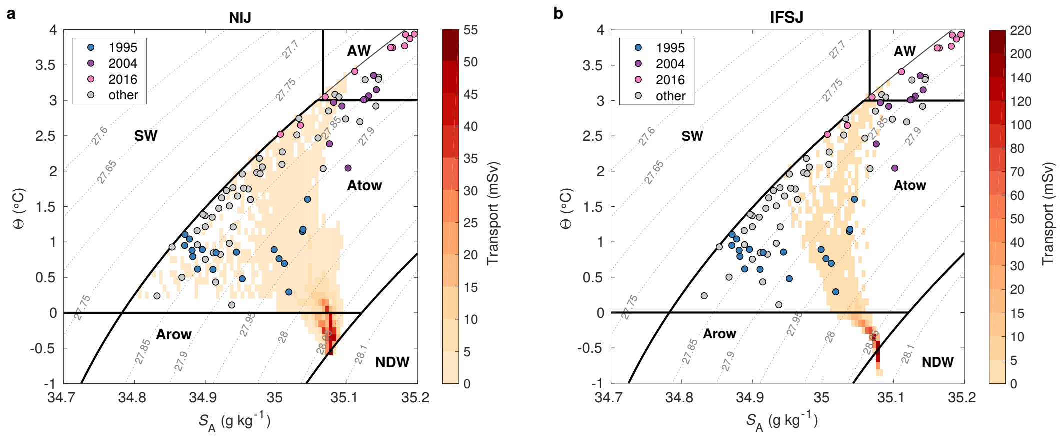

Figure 14. Hydrographic properties of the winter mixed layers on the north Iceland shelf exceeding overflow water density (circles colored according to the year of observation) in relation to the mean volume transport of overflow water in the a) NIJ and b) IFSJ displayed by temperature/salinity class (see color bar). The gray contours are density. The volume transport in the NIJ is an average of nine occupations at the Hornbanki section (Semper et al., 2019), while the transport in the IFSJ is an average of seven transects between northeast Iceland and the Faroe Islands (Semper, Pickart, Våge, Larsen, et al., 2020). Water masses are separated by thick black lines; their acronyms are: AW = Atlantic Water; Atow = Atlantic-origin water; Arow = Arctic-origin water; NDW = Nordic Seas Deep Water; SW = Surface Water.

tent with the observed salinity in the NIJ (Semper et al., 2019). Our observations indicate that dense-water formation on the north Iceland shelf is rare, in direct contradiction to the notion that the Iceland shelf is a major source to the NIJ as inferred from the numerical simulations by Garcia-Quintana et al. (2021).

The contrasting hydrographic properties of the dense mixed layers in 1995 versus those in 2004 and 2016 indicate that the water mass transformation occurred under different conditions. The winter of 1995 was characterized by stronger and more frequent northerly winds over the Nordic Seas than previously observed, leading to low air temperatures in Iceland (Malmberg & Jónsson, 1997; Valdimarsson & Malmberg, 1999). The influence of Arctic waters north of Iceland was substantial (Malmberg & Jónsson, 1997), while the heat transport of the NIIC was reduced and the Atlantic Water fraction was at a minimum of 36 % (Jónsson & Valdimarsson, 2012b). These extremely cold conditions favored local formation of overflow water. By contrast, the winter of 2004 followed the highest measured Atlantic Water inflow in the NIIC in 2003, when the flow was composed of 76 % Atlantic Water (Jónsson & Valdimarsson, 2012b). This high 2003 inflow was likely driven by intensified winds southwest of Iceland caused by the strengthening and westward shift of the Icelandic Low (Zhao et al., 2018). The strong Atlantic Water inflow brought large amounts of heat and salt onto the north Iceland shelf. While some heat was lost to the atmosphere during fall, the high salinity was likely reduced at a slower rate and facilitated densification and local formation of relatively saline overflow water the following winter. The proportion of Atlantic Water in the NIIC in 2015 was very high as well, and the same mechanism likely led to the very warm and saline overflow water on the shelf the following winter. According to Jónsson & Valdimarsson (2012b), in most winters the proportion of Atlantic Water in the NIIC varies between 53 and 67 %, so the winters of 1995 and 2004 were exceptional on opposite ends of this range. This suggests that the Atlantic Water fraction of the NIIC may dictate whether overflow water is formed on the north Iceland shelf and also determine its final properties.

7 Conclusions

Using hydrographic/velocity data from a high-resolution shipboard survey from September 2011, in combination with historical hydrographic measurements as well as satellite and surface drifter data, we investigated the evolution and transformation of the NIIC along the north Iceland shelf. The current generally follows the shelf break, except in the region of complex bathymetry near the Kolbeinsey Ridge, where the NIIC is deflected toward the coast along what can be considered an inner shelf break. The volume transport estimates and surface drifter data demonstrate that portions of the current recirculate in Denmark Strait and also west of the Kolbeinsey Ridge, consistent with previous studies. At the Hornbanki transect, approximately 300 km northeast of Denmark Strait, we estimated a transport of 1.6 ± 0.4 Sv, using absolute geostrophic velocity from the high-resolution hydrographic/velocity survey. This is within the range of earlier estimates, which are available for this section from disparate data sets and methods. The transport of the NIIC diminished significantly northeast of Iceland, and what remained of the current merged with the Atlantic Water inflow east of Iceland in fall 2011. However, we note that the current's eastward extent may vary seasonally and interannually; further investigation is needed to conclusively determine the ultimate fate of the NIIC.

The region northeast of Iceland is prone to baroclinic instability due to the steep bathymetry and enhanced velocities of the NIIC. Such instability facilitates the formation of eddies, which divert heat and salt from the shelf into the Iceland Sea. This process may contribute to the reduction of the volume transport of the NIIC, as some of the water exchanged with the Iceland Sea is likely overflow water, which is not considered in the transport estimate. EKE inferred from satellite altimetry and surface drifters, as well as sea surface temperature variability, revealed enhanced eddy activity in this region – in particular during winter. The co-location of this region with the emergence of the NIJ is an intriguing finding that deserves further exploration. Our observations are consistent with the simulations from the idealized model of Våge et al. (2011), who hypothesized the existence of a dynamical link between the NIIC and the formation of the NIJ.

The properties of the NIIC are modified along its entire pathway from Denmark Strait to east of Iceland. Considering all available historical hydrographic measurements, we estimate that the core of the current is freshened by approximately 0.02–0.03 g kg^{-1} per 100 km and cooled by 0.3 °C per 100 km in both summer and winter. The mixing with cold, fresh offshore waters along the NIIC's pathway appears to be the dominant mechanism that modifies the current, rather than air-sea interaction.

While dense overflow water is present on the north Iceland shelf year-round, especially in the vicinity of the shelf break, local formation of overflow water occurred only in approximately 11 % of all winter profiles over the period 1980–2016, mainly before the mid-1990s. The hydrographic properties of the water transformed on the shelf match the lighter portion of the NIJ and occasionally the IFSJ. Dense water formed on the north Iceland shelf may thus contribute to the shallower component of these slope currents. However, most of the more recent dense mixed layers were recorded during three particular winters that coincided with unusually low and high proportions of Atlantic Water in the NIIC.

The importance of the NIIC's heat and salt transport for the local climate and ecosystem is well known (e.g., Jónsson & Valdimarsson, 2012b). Previous studies have also suggested that there is a direct link between the NIIC and the NIJ, implying a significant influence of the NIIC on the northern extremity of the AMOC and thus large-scale climate (Våge et al., 2011; Pickart et al., 2017). Our results indicate that overturning on the north Iceland shelf may only sporadically supply the NIJ. Nevertheless, enhanced eddy kinetic energy in the region where the NIJ emerges suggests that the NIIC may play a key role for the dynamics of the NIJ and thus the overturning circulation in the Nordic Seas.

Acknowledgments

This research was supported by the European Union's Horizon 2020 research and innovation programme under the Marie Skłodowska-Curie grant agreement No 101022251 (S. Semper), the Trond Mohn Foundation Grant BFS2016REK01 (S. Semper and K. Våge), and the U.S. National Science Foundation Grants OCE-1558742 and OCE-1259618 (R. S. Pickart). The authors thank two anonymous reviewers for their insightful comments, which improved the manuscript. We also thank Ailin Brakstad for sharing an updated version of the historical hydrographic data set north of Iceland, which is available upon request from the corresponding author. The references to the individual data sets can be found in Huang et al. (2020). The hydrographic/velocity data are available in PANGAEA with the identifiers 10.1594/PANGAEA.919516, 10.1594/PANGAEA.919515, 10.1594/PANGAEA.903535, and 10.1594/PANGAEA.919569 and on `http://kogur.whoi.edu`. The near-surface drifter data are archived and distributed by the Atlantic Oceanographic and Meteorological Laboratory of the National Oceanic and Atmospheric Administration (AOML/NOAA; `https://www.aoml.noaa.gov/phod/gdp/mean_velocity.php`). The satellite sea surface height and sea surface temperature data are distributed by the E.U. Copernicus Marine Service Information (`http://marine.copernicus.eu`, product identifiers SEALEVEL_GLO_PHY_L3_REP_OBSERVATIONS_008_062 and SST_GLO_SST_L4_REP_OBSERVATIONS_010_024).

References

Amante, C., & Eakins, B. (2009). ETOPO1 1 arc-minute global relief model: Procedures, data sources, and analysis. *NOAA Technical Memorandum NESDIS NGDC-24*, 25. Retrieved from `https://www.ngdc.noaa.gov/mgg/global/relief/ETOPO1/docs/ETOPO1.pdf` doi: 10.1594/PANGAEA.769615

Årthun, M., Kolstad, E. W., Eldevik, T., & Keenlyside, N. S. (2018). Time scales and sources of European temperature variability. *Geophysical Research Letters*, *45*(8), 3597–3604. doi: 10.1002/2018GL077401

Astthorsson, O. S., Gislason, A., & Jónsson, S. (2007). Climate variability and the Icelandic marine ecosystem. *Deep-Sea Research Part II: Topical Studies in Oceanography*, *54*(23-26), 2456–2477. doi: 10.1016/j.dsr2.2007.07.030

Astthorsson, O. S., & Vilhjálmsson, H. (2002). Iceland shelf LME: Decadal assessment and resource sustainability. In K. Sherman & H. R. Skjoldal (Eds.), *Large marine ecosystems of the north atlantic. changing states and sustainability* (pp. 219–243). Amsterdam: Elsevier science. doi: 10.1016/S1570-0461(02)80059-3

Behrens, E., Våge, K., Harden, B., Biastoch, A., & Böning, C. W. (2017). Composition and variability of the Denmark Strait Overflow Water in a high-resolution numerical model hindcast simulation. *Journal of Geophysical Research: Oceans*, *122*, 2830–2846. doi: 10.1002/2016JC012264.

Bracco, A., Pedlosky, J., & Pickart, R. S. (2008). Eddy formation near the west coast of Greenland. *Journal of Physical Oceanography*, *38*(9), 1992–2002. doi: 10.1175/2008JPO3669.1

Brakstad, A., Våge, K., Håvik, L., & Moore, G. W. K. (2019). Water mass transformation in the Greenland Sea during the period 1986–2016. *Journal of Physical Oceanography*, *49*(1), 121–140. doi: 10.1175/JPO-D-17-0273.1

Casanova-Masjoan, M., Pérez-Hernández, M. D., Pickart, R. S., Valdimarsson, H., Ólafsdóttir, S. R., Macrander, A., … Hernández-Guerra, A. (2020). Alongstream, seasonal and interannual variability of the North Icelandic Irminger Current and

East Icelandic Current around Iceland. *Journal of Geophysical Research: Oceans*, *125*, e2020JC016283. doi: 10.1029/2020JC016283
Chafik, L., & Rossby, T. (2019). Volume, heat, and freshwater divergences in the subpolar North Atlantic suggest the Nordic Seas as key to the state of the meridional overturning circulation. *Geophysical Research Letters*, *46*(9), 4799–4808. doi: 10.1029/2019GL082110
Chérubin, L., Carton, X., Paillet, J., Morel, Y., & Serpette, A. (2000). Instability of the Mediterranean Water undercurrents southwest of Portugal: Effects of baroclinicity and of topography. *Oceanologica Acta*, *23*(5), 551–573. doi: 10.1016/S0399-1784(00)01105-1
Corlett, W. B., & Pickart, R. S. (2017). The Chukchi slope current. *Progress in Oceanography*, *153*, 50–65. Retrieved from `http://dx.doi.org/10.1016/j.pocean.2017.04.005` doi: 10.1016/j.pocean.2017.04.005
de Jong, M. F., Søiland, H., Bower, A. S., & Furey, H. H. (2018). The subsurface circulation of the Iceland Sea observed with RAFOS floats. *Deep-Sea Research Part I: Oceanographic Research Papers*, *141*, 1–10. doi: 10.1016/j.dsr.2018.07.008
Dickson, R. R., & Brown, J. (1994). The production of North Atlantic Deep Water: sources, rates, and pathways. *Journal of Geophysical Research*, *99*(C6), 12319–12341. doi: 10.1029/94jc00530
Egbert, G. D., & Erofeeva, S. Y. (2002). Efficient inverse modeling of barotropic ocean tides. *Journal of Atmospheric and Oceanic Technology*, *19*(2), 183–204. doi: 10.1175/1520-0426(2002)019⟨0183:EIMOBO⟩2.0.CO;2
Fogelqvist, E., Blindheim, J., Tanhua, T., Østerhus, S., Buch, E., & Rey, F. (2003). Greenland-Scotland overflow studied by hydro-chemical multivariate analysis. *Deep-Sea Research Part I: Oceanographic Research Papers*, *50*, 73–102. doi: 10.1016/S0967-0637(02)00131-0
Garcia-Quintana, Y., Grivault, N., Hu, X., & Myers, P. G. (2021). Dense water formation on the Icelandic shelf and its contribution to the North Icelandic Jet. *Journal of Geophysical Research: Oceans*, *126*(e2020JC016951). doi: 10.1029/2020jc016951
Gelderloos, R., Katsman, C. A., & Drijfhout, S. S. (2011). Assessing the roles of three eddy types in restratifying the Labrador Sea after deep convection. *Journal of Physical Oceanography*, *41*(11), 2102–2119. doi: 10.1175/JPO-D-11-054.1
Hansen, B., & Østerhus, S. (2000). North Atlantic-Nordic Seas exchanges. *Progress in Oceanography*, *45*(2), 109–208. doi: 10.1016/S0079-6611(99)00052-X
Harden, B., Pickart, R. S., Valdimarsson, H., Våge, K., de Steur, L., Richards, C., ... Hattermann, T. (2016). Upstream sources of the Denmark Strait Overflow: Observations from a high-resolution mooring array. *Deep-Sea Research Part I: Oceanographic Research Papers*, *112*, 94–112. doi: 10.1016/j.dsr.2016.02.007
Håvik, L., Pickart, R. S., Våge, K., Torres, D., Thurnherr, A. M., Beszczynska-Möller, A., ... von Appen, W.-J. (2017). Evolution of the East Greenland Current from Fram Strait to Denmark Strait: Synoptic measurements from summer 2012. *Journal of Geophysical Research: Oceans*, *122*(3), 1974–1994. doi: 10.1002/2016JC012228
Håvik, L., Våge, K., Pickart, R. S., Harden, B., von Appen, W.-J., Jónsson, S., & Østerhus, S. (2017). Structure and variability of the shelfbreak East Greenland current north of Denmark Strait. *Journal of Physical Oceanography*, *47*(10), 2631–2646. doi: 10.1175/JPO-D-17-0062.1
Helland-Hansen, B., & Nansen, F. (1909). The Norwegian Sea: its physical oceanography based upon the Norwegian researches, 1900-1904. *Report on Norwegian Fishery and Marine Investigations*, *2*(2), 390. doi: 10.2307/1776951
Hersbach, H., Bell, B., Berrisford, P., Hirahara, S., Horányi, A., Muñoz-Sabater, J., ... Thépaut, J. N. (2020). The ERA5 global reanalysis. *Quarterly Journal of the*

Royal Meteorological Society, *146*(730), 1999–2049. doi: 10.1002/qj.3803

Huang, J., Pickart, R. S., Huang, R. X., Lin, P., Brakstad, A., & Xu, F. (2020). Sources and upstream pathways of the densest overflow water in the Nordic Seas. *Nature Communications*, *11*(5389). doi: 10.1038/s41467-020-19050-y

Huang, J., Pickart, R. S., Valdimarsson, H., Lin, P., Spall, M. A., & Xu, F. (2019). Structure and variability of the North Icelandic Jet from two years of mooring data. *Journal of Geophysical Research: Oceans*, *124*. doi: 10.1029/2019JC015134

IOC, SCOR, & IAPSO. (2010). The international thermodynamic equation of seawater - 2010: Calculation and use of thermodynamic properties. *Intergovernmental Oceanographic Commission, Manuals and Guides No. 56, UNESCO*, 196 pp. Retrieved from `http://www.teos-10.org`

Isachsen, P. E., Koszalka, I., & LaCasce, J. H. (2012). Observed and modeled surface eddy heat fluxes in the eastern Nordic Seas. *Journal of Geophysical Research: Oceans*, *117*(8), 1–10. doi: 10.1029/2012JC007935

Isachsen, P. E., Mauritzen, C., & Svendsen, H. (2007). Dense water formation in the Nordic Seas diagnosed from sea surface buoyancy fluxes. *Deep-Sea Research Part I: Oceanographic Research Papers*, *54*(1), 22–41. doi: 10.1016/j.dsr.2006.09.008

Jochumsen, K., Schnurr, S. M., & Quadfasel, D. (2016). Bottom temperature and salinity distribution and its variability around Iceland. *Deep-Sea Research Part I: Oceanographic Research Papers*, *111*, 79–90. Retrieved from `http://dx.doi.org/10.1016/j.dsr.2016.02.009` doi: 10.1016/j.dsr.2016.02.009

Jónsson, S. (2007). Volume flux and fresh water transport associated with the East Icelandic Current. *Progress in Oceanography*, *73*(3-4), 231–241. doi: 10.1016/j.pocean.2006.11.003

Jónsson, S., & Valdimarsson, H. (2004). A new path for the Denmark Strait overflow water from the Iceland Sea to Denmark Strait. *Geophysical Research Letters*, *31*(3), L03305. doi: 10.1029/2003GL019214

Jónsson, S., & Valdimarsson, H. (2005). The flow of Atlantic Water to the north Icelandic shelf and its relation to the drift of cod larvae. *ICES Journal of Marine Science*, *62*(7), 1350–1359. doi: 10.1016/j.icesjms.2005.05.003

Jónsson, S., & Valdimarsson, H. (2012a). Hydrography and circulation over the southern part of the Kolbeinsey Ridge. *ICES Journal of Marine Science*, *69*(7), 1255–1262. doi: 10.1093/icesjms/fss101

Jónsson, S., & Valdimarsson, H. (2012b). Water mass transport variability to the north Icelandic shelf, 1994-2010. *ICES Journal of Marine Science*, *69*(5), 809–815. doi: 10.1093/icesjms/fst034

Laurindo, L. C., Mariano, A. J., & Lumpkin, R. (2017). An improved near-surface velocity climatology for the global ocean from drifter observations. *Deep-Sea Research Part I: Oceanographic Research Papers*, *124*, 73–92. doi: 10.1016/j.dsr.2017.04.009

Lilly, J. M., Rhines, P. B., Schott, F., Lavender, K., Lazier, J., Send, U., & D'Asaro, E. (2003). Observations of the Labrador Sea eddy field. *Progress in Oceanography*, *59*(1), 75–176. doi: 10.1016/j.pocean.2003.08.013

Logemann, K., Ólafsson, J., Snorrason, Á., Valdimarsson, H., & Marteinsdóttir, G. (2013). The circulation of Icelandic waters - A modelling study. *Ocean Science*, *9*(5), 931–955. doi: 10.5194/os-9-931-2013

Lorbacher, K., Dommenget, D., Niiler, P. P., & Köhl, A. (2006). Ocean mixed layer depth: A subsurface proxy of ocean-atmosphere variability. *Journal of Geophysical Research: Oceans*, *111*(7), 1–22. doi: 10.1029/2003JC002157

Macrander, A., Valdimarsson, H., & Jónsson, S. (2014). Improved transport estimate of the East Icelandic Current 2002-2012. *Journal of Geophysical Research: Oceans*, *119*(6), 3407–3424. doi: 10.1002/2013JC009517

Malmberg, S.-A., & Jónsson, S. (1997). Timing of deep convection in the Greenland and Iceland Seas. *ICES Journal of Marine Science*, *54*(3), 300–309. doi: 10.1006/

jmsc.1997.0221

Malmberg, S.-A., & Kristmannsson, S. S. (1992). Hydrographic conditions in Icelandic waters, 1980-1989. *ICES mar. Sci. Symp.*, *195*, 76–92.

Mastropole, D., Pickart, R. S., Valdimarsson, H., Våge, K., Jochumsen, K., & Girton, J. B. (2017). On the hydrography of Denmark Strait. *Journal of Geophysical Research: Oceans*, *122*, 306–321. doi: 10.1002/2016JC012007

Mauritzen, C. (1996). Production of dense overflow waters feeding the North Atlantic across the Greenland-Scotland Ridge. Part 1: Evidence for a revised circulation scheme. *Deep-Sea Research Part I: Oceanographic Research Papers*, *43*(6), 769–806. doi: 10.1016/0967-0637(96)00037-4

Meincke, J. (1974). Overflow '73 - Large-scale features of the overflow across the Iceland-Faroe Ridge. *ICES report CM-1974/C:7*.

Moore, G. W. K., Våge, K., Pickart, R. S., & Renfrew, I. A. (2015). Decreasing intensity of open-ocean convection in the Greenland and Iceland seas. *Nature Climate Change*, *5*(9), 877–882. doi: 10.1038/nclimate2688

Mork, K. A., Skagseth, Ø., & Søiland, H. (2019). Recent warming and freshening of the Norwegian Sea observed by Argo data. *Journal of Climate*, *32*(12), 3695–3705. doi: 10.1175/JCLI-D-18-0591.1

Nilsen, J. E. Ø., & Falck, E. (2006). Variations of mixed layer properties in the Norwegian Sea for the period 1948-1999. *Progress in Oceanography*, *70*(1), 58–90. doi: 10.1016/j.pocean.2006.03.014

Østerhus, S., Woodgate, R., Valdimarsson, H., Turrell, B., De Steur, L., Quadfasel, D., … Berx, B. (2019). Arctic Mediterranean exchanges: A consistent volume budget and trends in transports from two decades of observations. *Ocean Science*, *15*(2), 379–399. doi: 10.5194/os-15-379-2019

Pacini, A., & Pickart, R. S. (2022). Meanders of the west greenland current near cape farewell. *Deep Sea Research Part I: Oceanographic Research Papers*, *179*, 103664. doi: https://doi.org/10.1016/j.dsr.2021.103664

Perkins, H., Hopkins, T. S., Malmberg, S. A., Poulain, P. M., & Warn-Varnas, A. (1998). Oceanographic conditions east of Iceland. *Journal of Geophysical Research: Oceans*, *103*(C10), 21531–21542. doi: 10.1029/98JC00890

Pickart, R. S., & Smethie, W. M. (1998). Temporal evolution of the deep western boundary current where it enters the sub-tropical domain. *Deep Sea Research Part I: Oceanographic Research Papers*, *45*(7), 1053–1083. doi: 10.1016/S0967-0637(97)00084-8

Pickart, R. S., Spall, M. A., Torres, D. J., Våge, K., Valdimarsson, H., Nobre, C., … Mastropole, D. (2017). The North Icelandic Jet and its relationship to the North Icelandic Irminger Current. *Journal of Marine Research*, *75*(5), 605–639. doi: 10.1357/002224017822109505

Pickart, R. S., Torres, D. J., & Clarke, R. A. (2002). Hydrography of the Labrador Sea during active convection. *Journal of Physical Oceanography*, *32*(2), 428–457. doi: 10.1175/1520-0485(2002)032⟨0428:HOTLSD⟩2.0.CO;2

Poulain, P.-M., Warn-Varnas, A., & Niiler, P. P. (1996). Near-surface circulation of the Nordic seas as measured by Lagrangian drifters. *Journal of Geophysical Research: Oceans*, *101*, 18237–18258. doi: 10.1029/96JC00506

Price, J. F., Weller, R. A., & Pinkel, R. (1986). Diurnal cycling: observations and models of the upper ocean response to diurnal heating, cooling, and wind mixing. *Journal of Geophysical Research*, *91*(6), 8411–8427. doi: 10.1029/jc091ic07p08411

Read, J. F., & Pollard, R. T. (1992). Water masses in the region of the Iceland-Færoes Front. *Journal of Physical Oceanography*, *22*, 1365–1378.

Richards, C. G., & Straneo, F. (2015). Observations of water mass transformation and eddies in the Lofoten Basin of the Nordic Seas. *Journal of Physical Oceanography*, *45*(6), 1735–1756. doi: 10.1175/JPO-D-14-0238.1

Rudels, B., Björk, G., Nilsson, J., Winsor, P., Lake, I., & Nohr, C. (2005). The interaction between waters from the Arctic Ocean and the Nordic Seas north of Fram Strait and along the East Greenland Current: Results from the Arctic Ocean-02 Oden expedition. *Journal of Marine Systems*, *55*(1-2), 1–30. doi: 10.1016/j.jmarsys.2004.06.008

Saberi, A., Haine, T. W. N., Gelderloos, R., Femke de Jong, M., Furey, H. H., & Bower, A. (2020). Lagrangian perspective on the origins of Denmark Strait overflow. *Journal of Physical Oceanography*, *50*(8), 2393–2414. doi: 10.1175/jpo-d-19-0210.1

Semper, S., Pickart, R. S., Våge, K., Larsen, K. M. H., Hátún, H., & Hansen, B. (2020). The Iceland-Faroe Slope Jet: A conduit for dense water toward the Faroe Bank Channel overflow. *Nature Communications*, *11*(5390). doi: 10.1038/s41467-020-19049-5

Semper, S., Pickart, R. S., Våge, K., Torres, D. J., & McRaven, L. (2020a). *CTD temperature and salinity profiles along five transects in NE Iceland / Iceland-Faroe ridge.* PANGAEA. Retrieved from `https://doi.pangaea.de/10.1594/PANGAEA.919516`

Semper, S., Pickart, R. S., Våge, K., Torres, D. J., & McRaven, L. (2020b). *Water velocity profiles from LADCP casts along five transects in NE Iceland / Iceland-Faroe ridge.* PANGAEA. Retrieved from `https://doi.pangaea.de/10.1594/PANGAEA.919515`

Semper, S., Våge, K., Pickart, R. S., Valdimarsson, H., Torres, D. J., & Jónsson, S. (2019). The emergence of the North Icelandic Jet and its evolution from northeast Iceland to Denmark Strait. *Journal of Physical Oceanography*, *49*(10), 2499–2521. doi: 10.1175/jpo-d-19-0088.1

Semper, S., Våge, K., Pickart, R. S., Valdimarsson, H., Torres, D. J., Jónsson, S., ... Danielsen, M. (2019). *Temperature, salinity and velocities on seven transects along the continental slope north of Iceland.* PANGAEA. Retrieved from `https://doi.org/10.1594/PANGAEA.903535`

Semper, S., Våge, K., Pickart, R. S., Valdimarsson, H., Torres, D. J., Jónsson, S., ... Danielsen, M. (2020). *Water velocity profiles in the transect Slétta from LADCP from several cruises.* PANGAEA. Retrieved from `https://doi.pangaea.de/10.1594/PANGAEA.919569`

Spall, M. A. (2010). Non-local topographic influences on deep convection: An idealized model for the Nordic Seas. *Ocean Modelling*, *32*(1-2), 72–85. doi: 10.1016/j.ocemod.2009.10.009

Stefánsson, U. (1962). North Icelandic Waters. *Rit Fiskideildar*, *3*.

Stefánsson, U., & Ólafsson, J. (1991). Nutrients and fertility of Icelandic waters. *Rit Fiskideildar*, *7*, 1–56.

Strass, V. H., Fahrbach, E., Schauer, U., & Sellmann, L. (1993). Formation of Denmark Strait overflow water by mixing in the East Greenland Current. *Journal of Geophysical Research*, *98*(C4), 6907–6919. doi: 10.1029/92JC02732

Swift, J. H., & Aagaard, K. (1981). Seasonal transitions and water mass formation in the Iceland and Greenland Seas. *Deep Sea Research*, *28A*(10), 1107–1129.

Thórdardóttir, T. (1984). Primary production north of Iceland in relation to water masses in May-June 1970-1980. *ICES CM-1984/L:20*, 17.

Thurnherr, A. (2010). A practical assessment of the errors associated with full-depth LADCP profiles obtained using Teledyne RDI Workhorse acoustic Doppler current profilers. *Journal of Atmospheric and Oceanic Technology*, *27*(7), 1215–1227. doi: 10.1175/2010JTECHO708.1

Thurnherr, A. (2018). *How to process LADCP data with the LDEO software* (Tech. Rep.). Retrieved from `ftp://ftp.ldeo.columbia.edu/pub/LADCP/UserManuals/LDEO_IX.pdf`

Tsubouchi, T., Våge, K., Hansen, B., Larsen, K. M. H., & Østerhus, S. (2021).

Increased ocean heat transport into the Arctic Mediterranean over the period 1993–2016. *Nature Climate Change*, *11*, 21–26. doi: 10.1038/s41558-020-00941-3

Våge, K., Moore, G. W. K., Jónsson, S., & Valdimarsson, H. (2015). Water mass transformation in the Iceland Sea. *Deep-Sea Research Part I: Oceanographic Research Papers*, *101*, 98–109. doi: 10.1016/j.dsr.2015.04.001

Våge, K., Papritz, L., Håvik, L., Spall, M. A., & Moore, G. W. K. (2018). Ocean convection linked to the recent ice edge retreat along east Greenland. *Nature Communications*, *9*(1). doi: 10.1038/s41467-018-03468-6

Våge, K., Pickart, R. S., Spall, M. A., Moore, G. W. K., Valdimarsson, H., Torres, D. J., ... Nilsen, J. E. Ø. (2013). Revised circulation scheme north of the Denmark Strait. *Deep-Sea Research Part I: Oceanographic Research Papers*, *79*, 20–39. doi: 10.1016/j.dsr.2013.05.007

Våge, K., Pickart, R. S., Spall, M. A., Valdimarsson, H., Jónsson, S., Torres, D. J., ... Eldevik, T. (2011). Significant role of the North Icelandic Jet in the formation of Denmark Strait overflow water. *Nature Geoscience*, *4*(10), 723–727. doi: 10.1038/ngeo1234

Våge, K., Semper, S., Valdimarsson, H., Jónsson, S., Pickart, R. S., & Moore, G. W. K. (in revision). Water mass transformation in the Iceland Sea: Contrasting two winters separated by four decades. *Deep Sea Research Part I: Oceanographic Research Papers*.

Valdimarsson, H., & Malmberg, S.-A. (1999). Near-surface circulation in Icelandic waters derived from satellite tracked drifters. *Rit Fiskideildar*, *16*, 23–39.

Voet, G., Quadfasel, D., Mork, K. A., & Søiland, H. (2010). The mid-depth circulation of the Nordic Seas derived from profiling float observations. *Tellus, Series A: Dynamic Meteorology and Oceanography*, *62*(4), 516–529. doi: 10.1111/j.1600-0870.2010.00444.x

von Appen, W.-J., Schauer, U., Hattermann, T., & Beszczynska-Möller, A. (2016). Seasonal cycle of mesoscale instability of the West Spitsbergen Current. *Journal of Physical Oceanography*, *46*(4), 1231–1254. doi: 10.1175/JPO-D-15-0184.1

Ypma, S. L., Brüggemann, N., Georgiou, S., Spence, P., Dijkstra, H. A., Pietrzak, J. D., & Katsman, C. A. (2019). Pathways and watermass transformation of Atlantic Water entering the Nordic Seas through Denmark Strait in two high resolution ocean models. *Deep-Sea Research Part I: Oceanographic Research Papers*, *145*, 59–72. doi: 10.1016/j.dsr.2019.02.002

Zhao, J., Yang, J., Semper, S., Pickart, R. S., Våge, K., Valdimarsson, H., & Jónsson, S. (2018). A numerical study of interannual variability in the North Icelandic Irminger Current. *Journal of Geophysical Research: Oceans*, *123*(12), 8994–9009. doi: 10.1029/2018JC013800